# A cryospectroscopic infrared and Raman study of the halogen bonding motif : complexes of the , , and with ethyne, propyne and 2-butyne


**Spectrochimica acta: part A: molecular and biomolecular spectroscopy** - ISSN 1386-1425 - 136(2015), p. 16-26
DOI: http://dx.doi.org/doi:10.1016/j.saa.2014.04.141
Handle: http://hdl.handle.net/10067/1235980151162165141

# A cryospectroscopic infrared and Raman study of the C-X···π halogen bonding motif : complexes of the $CF_3Cl$ , $CF_3Br$ , and $CF_3I$ with ethyne , propyne and 2-butyne.

N. Nagels, W.A. Herrebout *

Department of Chemistry, University of Antwerp, Groenenborgerlaan 171,

B-2020 Antwerp, Belgium

**Abstract**

Experimental information on the C-X···π halogen bonding motif was obtained by studying the formation of molecular complexes of $CF_3Cl$, $CF_3Br$ and $CF_3I$ with ethyne, propyne and 2-butyne in liquid krypton, using FTIR and Raman spectroscopy. For $CF_3Br$, experimental evidence was found for the formation of 1:1 complexes with propyne and 2-butyne only, while for $CF_3I$ spectroscopic features confirming the existence of the halogen bonded complexes were observed for ethyne, propyne and 2-butyne. In addition, at higher concentrations of $CF_3I$ and 2-butyne, weak absorptions due to a 2:1 complex were also observed. The experimental complexation enthalpies, obtained by using spectra recorded at temperatures between 120 K and 140 K, are -5.9(3) kJ $mol^{-1}$ for $CF_3I$•ethyne, -5.6(3) $kJmol^{-1}$ for $CF_3Br$•propyne, -8.1(2) kJ $mol^{-1}$ for $CF_3I$•propyne, -7.3(2) kJ $mol^{-1}$ for $CF_3Br$•2-butyne, -10.9(2) kJ $mol^{-1}$ for $CF_3I$•2-butyne and -20.9(7) kJ $mol^{-1}$ for $(CF_3I)_2$•2-butyne. The experimental study is supported by theoretical data obtained from ab initio calculations at the MP2/aug-cc-pVDZ(-PP) and MP2/aug-cc-pVTZ(-PP) levels, and Monte Carlo Free Energy Perturbation (MC-FEP) simulations. The experimental and theoretical values on the C-X···π halogen-bonding motifs studied are compared with previously reported data for the complexes with ethene and propene and with preliminary results obtained for benzene and toluene.

* corresponding author.

*Tel.* +32-3-2653373 , Fax. +32-3-2653205,

*Email address:* wouter.herrebout@ua.ac.be

**Keywords**: halogen bonding motifs, infrared, Raman, C-X···π halogen bonding, cryosolutions

**Highlights:**

° Infrared and Raman experiments of solutions in liquid krypton lead to new experimental information on the C-X···π halogen bonding motif**.**

° Experimental information on the stoichiometry and the complexation enthalpy of the complexes of $CF_3I$ and $CF_3Br$ with ethyne, propyne and 2-butyne, is obtained from concentration and temperature studies.

° The experimental studies are supported by the high level ab initio calculations and Monte Carlo Free Energy Perturbation simulations. An excellent agreement between experiment and theory is observed.

° Comparison of the data obtained for alkynes with data reported for alkenes and aromatic model systems lead to a more complete understanding of the C-X···π halogen bonding motif.

**Graphical Abstract**

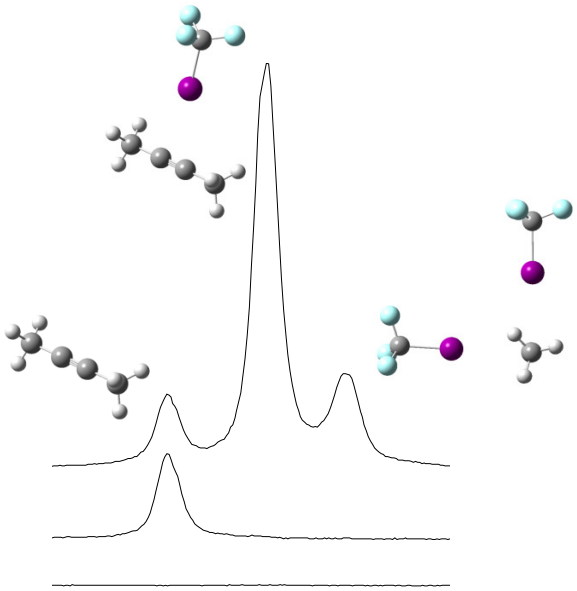

## 1. Introduction

Triggered by the growing number of applications in the field of crystal engineering [1,2] , supramolecular chemistry [3,4] and drug design [5,6] and by their role in several biochemical processes [7,8] and molecular recognition systems [9,10] , C-X···Y halogen bonds have recently gained large interest amongst experimentalists and theoreticians.

The growing awareness of halogen bonding is evident from the numerous highlights, reviews and perspectives published in the last few years [11-16]. However, despite the growing interest in the applications of halogen bonding, experimental data describing the intrinsic properties of halogen bonds appearing in binary complexes is still limited. As a result, reliable data allowing the assessment of the different computational methodologies used to model their role in various applications remains scarce. In a contribution to fill this gap, Walker et al. [17,18] have recently reported the results of a systematic study in which the structural data for a series of complexes formed between trifluoroiodomethane, $CF_3I$, and a series of Lewis bases including $N_2$, CO, Kr, ammonia, trimethyl amine and ethene was obtained using Fourier transform microwave experiments. The experimental data reported is in line with the microwave studies on the complexes formed between ammonia and $CF_3Cl$ reported by Caminati et al. [19] and complement recent experimental data obtained by performing systematic infrared and Raman spectroscopic studies [20-23] of the molecular complexes of the trifluorohalomethanes $CF_3Cl$, $CF_3Br$ and $CF_3I$ with a variety of model Lewis bases formed in cryogenic solutions, i.e. in liquid argon (LAr), krypton (LKr), and/or xenon (LXe). In contrast to the molecular beams used in the microwave studies, these solutions allow the complexes to be studied under equilibrium conditions, at temperatures between 88 and 228 K. By applying the necessary corrections for thermal and solvent effects, and by using the Van 't Hoff isochore, these chemical equilibrium experiments thus allow the experimental determination of the complexation enthalpy.

The experimental observation of 1:1 complexes between ethene, propene and $CF_3I$ formed in cryosolutions and in molecular beams illustrate that not only heteroatoms can be involved in the formation of a halogen bond, but that also π-systems can function as electron donors. The results thus strongly support recent PDB protein database studies suggesting that C-X···π halogen bonds involving organic halogen atoms and the aromatic side chains of peptides can play a dominating role in biomolecules and in protein ligand interactions [24-26].

To be able to rationalize the general trends observed when passing from one Lewis base to another, and to be able to rationalize similarities and differences observed when passing from alkenes to alkynes, in this paper we report on an experimental, infrared and Raman, study of the halogen bonded complexes of $CF_3X$ (X = Cl, Br and I) with ethyne, propyne and 2-butyne dissolved in LKr. The results presented will be compared with the data on the halogen bonded complexes with ethene and propene [21]

and with preliminary data obtained for the aromatic model systems benzene and toluene [27]. The data reported are in line with and support the general ideas put forward by Shishkin et al. [28] in their study of C-Cl···π bonding motifs inside supramolecular nanotubes of hexaethynylhexamethoxy-[6]pericyclyne.

## 2. Experimental and Computational Details

The samples of 2-butyne (99%) and trifluoroiodomethane ($CF_3I$, 99%) were purchased from Sigma Aldrich. The samples of propyne (98%) and chlorotrifluoromethane ($CF_3Cl$, 99%) were acquired from Praxair. The sample of bromotrifluoromethane ($CF_3Br$, 99%) was obtained from Pfaltz & Bauer. Ethyne was synthesized in small amounts by hydrolyzing $CaC_2$ with $H_2O$ and was purified by pumping the reaction mixture through a 2-propanol slush (180 K), followed by fractionation on a low-temperature, low-pressure fractionation column [29,30]. To ensure sufficient solubility of all listed compounds krypton (Air Liquide, 99.9995%) was used as solvent gas.

Infrared spectra were recorded on a Bruker IFS 66v Fourier transform spectrometer. A Globar source was used in combination with a Ge/KBr beam splitter and a $LN_2$-cooled broad band MCT detector. The interferograms were averaged over 500 scans, Blackman-Harris three-term apodized and Fourier transformed with a zero filling factor of 4, to yield spectra with a resolution of 0.5 $cm^{-1}$. A description of the experimental set-up used to investigate the solutions in liquid noble gases has been given before [31-33]. A liquid cell equipped with wedged Si windows and a path length of 1 cm was used.

Raman spectra were recorded using a Trivista 557 spectrometer consisting of a double $f$ = 50 cm monochromator equipped with 300/1500/2000 lines $mm^{-1}$ gratings and a $f$ = 70 cm spectrograph equipped with 500/1800/2400 lines $mm^{-1}$ gratings and a back-end illuminated $LN_2$ cooled CCD detector. The 514.5 nm line of a Spectra-Physics argon ion laser was used for Raman excitation, and the power of the incident laser beam was set to 0.8 W. Frequencies were calibrated using Ne emission lines, and are expected to be accurate to 0.5 $cm^{-1}$. The full widths at half height of the most intense Ne lines studied, typically varied between 0.5 and 0.6 $cm^{-1}$. The experimental set-up, which includes a liquid cell equipped with four quartz windows at right angles, and the filling procedures have been described before [34,35].

Geometries and harmonic vibrational frequencies of monomers and complexes were obtained from ab initio calculations at the MP2/aug-cc-pVDZ(-PP) level, using Gaussian09 [36]. A more reliable complexation energy was derived from a single point ab initio calculation at the MP2/aug-cc-pVTZ(-PP) level. Corrections for BSSE were accounted for using CP-corrected gradient techniques. The standard aug-cc-pVD(T)Z basis sets were used for hydrogen, carbon, fluorine and chlorine atoms. For bromine and iodine atoms, the aug-cc-pVD(T)Z-PP basis sets were used, which include small-core energy-consistent relativistic pseudopotentials (PP). The combination of the MP2 methodology and the aug-cc-

pVD(T)Z(-PP) basis sets has resulted in satisfactory predictions of halogen bonded complexes before [20-23,37].

Solvation Gibbs energies $\Delta_{sol}G$ were obtained by correcting the calculated complexation energies for solvent and thermal influences. Corrections for solvent effects were obtained from Monte Carlo Free Energy Perturbation (MC-FEP) simulations [38], using a locally modified version of BOSS4.1 [39,40]. Corrections for thermal effects were estimated by applying statistical thermodynamic calculations [41,42].

## 3. Results and Discussion

### 3.1. Ab initio calculations

The MP2/aug-cc-pVDZ(-PP) equilibrium geometries for the complexes of $CF_3X$ with ethyne, propyne and 2-butyne are shown schematically in Fig. 1. The characteristic structural parameters are summarized in Tables 1, 2 and 3. For ethyne and 2-butyne, the calculations converged to a structure with $C_s$ symmetry, while for propyne the symmetry of the resulting complex was $C_1$. For the complexes with 2-butyne, different orientations of the methyl groups are observed, in which the hydrogen atoms are in an eclipsed ($CF_3Cl$) or in a staggered configuration ($CF_3Br$, $CF_3I$). These changes are explained by the fact that, although the complex is significantly weaker, the methyl groups in the complex with $CF_3Cl$ tend to be in closer contact with the fluorine atoms of the $CF_3X$ moiety, and thus can lead to secondary stabilizations.[9d, 12] The presence of weak C-H···F interactions in the complexes studied also is illustrated by the deviations from linearity observed for the C-X···π halogen bonds formed with propyne, the resulting values being close to 180 degrees for ethyne and 2-butyne, and being in the order of 171 to 175 degrees for propyne, respectively.

We have recently shown [20-23] that for complexes involving the trifluorohalomethanes, information on the strength of the interaction can be derived by comparing the interatomic distances between the accepting and donating atoms $R_{eq}$ and the sum of the respective van der Waals radii $R_{VdW}$. The values for the (C-)X···π distances obtained by calculating the distance between the interacting halogen atom and the midpoint of the carbon-carbon triple bond, the values for the distance ratios $R_p = R_{eq} / R_{VdW}$, and the MP2 complexation energies are summarized in Table 4. Inspection of the data shows that for all alkynes studied, the ratios obtained for the different Lewis bases slightly decrease from $CF_3Cl$ to $CF_3I$, the limiting values being 0.97 and 0.91 for ethyne, 0.96 and 0.88 for propyne, and 0.93 and 0.85 for 2-butyne. These trends strongly correlate with those observed for the MP2/aug-cc-pVDZ(-PP) and MP2/aug-cc-pVTZ(-PP) complexation energies, showing that for all Lewis bases studied the complexation energies increase by 70-75 % while substituting chlorine by iodine and by 85-90 % while passing from ethyne to 2-butyne. The trends also are in line with the increase in size and depth of the respective σ-holes

appearing for $CF_3Cl$, $CF_3Br$ and $CF_3I$ [43] and with the idea that methyl groups act as electron donors and thus tend to increase the electron donating capacity of the Lewis base [29,30]. To complement the data reported and to shed further light onto the nature of the interactions present, Table 4 also includes the values for the van der Waals penetration distance $d_P$ and the netto charge transfer from the Lewis base to the Lewis acid. The penetration distance $d_P$ is defined as $d_P = R_{VdW} - R_{eq}$ and, in a first approximation, can be used [44] to evaluate if, apart from electrostatic contributions, a donor-acceptor character is present in the bonding, with the boundary for a significant contribution being $d_P \geq 0.1$ Å. The netto charge transfer is calculated by comparing the atomic partial charges obtained by fitting the electrostatic potential using the CHelpG algorithm [45].

For the complexes of $CF_3Cl$ with ethyne and propyne, the value for the penetration distance is close to or significantly smaller than the boundary setting of 0.1 Å. For both complexes, the effect of charge transfer can therefore be minimized. In contrast, for all other complexes a substantial penetration distance suggesting a significant contribution due to charge transfer is observed. It can also be seen that the penetration distance gradually increases when passing from ethyne to 2-butyne and when passing from $CF_3Cl$ to $CF_3I$. The general trends observed for the penetration distances $d_P$ and the increase of the donor-acceptor character derived from them are in excellent agreement with the changes observed for the netto charge transfers, the smallest and largest values being a mere -0.026e for ethyne•$CF_3Cl$ and -0.096e for 2-butyne•$CF_3I$, and compare favorably with the other data discussed above.

The MP2/aug-cc-pVDZ(-PP) harmonic vibrational frequencies and infrared intensities obtained for the monomers and for the different complexes under study are listed in Tables S1-S9 of the ESI. The characteristic vibrations for the complexes with ethyne, propyne and 2-butyne are summarized in Tables 5, 6 and 7. This data will be used to rationalize the different trends and complexation shifts observed in the experimental studies, and will be referred to in the following paragraphs whenever necessary.

It will be shown below that evidence for the formation of a 2:1 complex, containing two molecules $CF_3I$ and a single molecule 2-butyne, is found in the experimental spectra. Theoretical information on this 2:1 complex was, therefore, also derived. The resulting equilibrium geometry is shown in Fig. 2. The more important vibrational frequencies of the 2:1 complex are compared with the corresponding values of the monomer and the 1:1 complex in Table 8. The angle between the two $CF_3I$ molecules in the 2:1 complex, with $C_1$ symmetry, is 86.74 °, which is close to 90°. Forcing the two $CF_3I$ molecules in a co-linear geometry resulted in three imaginary frequencies, indicating that such a structure does not refer to a minimum I nthe potential energy surface. The observation of a geometry with two nearly orthogonal halogen bonds is in line with data reported for the 2:1 complexes formed between $BF_3$ and propyne [29,30]. Also for this type of complex, two interactions were observed in a nearly orthogonal position, the angle between the two $\pi\cdots B$ bonds being approximately 107.5°. The slightly larger value obtained for this type of complex and the small differences with the complex studied here, to

our opinion, are related to the repulsion appearing when the two $BF_3$ molecules approach the Lewis base and tend to overlap in a close to 90° setting.

Analogous to the 2:1 complex of $CF_3I$ with propene [21], and to the 2:1 complex of $BF_3$ with propyne [29,30] also for the 2:1 complex of $CF_3I$ with 2-butyne, a weak anti-cooperative effect is found in which the first halogen bond weakens the second one and vice versa. The effect of this phenomenon is clearly visible from the complexation energies for the 1:1 and 2:1 complexes and from the small changes in the halogen bond lengths. The value of the interaction energy for the 2:1 complex is calculated to be -39.5 kJ $mol^{-1}$, which is some 5 % smaller than twice the value of -20.0 kJ $mol^{-1}$ for the 1:1 complex. The values for the halogen bond lengths for the 1:1 and 2:1 complex are 3.294 and 3.311 Å, respectively.

### 3.2. Statistical Thermodynamics and MC-FEP Simulations

To allow comparison of theory and experiment, LKr complexation enthalpies $\Delta H°$(LKr,calc) were predicted by correcting the MP2/aug-cc-pVTZ(-PP) complexation energies $\Delta E$(calc) for solvent, thermal and zero-point vibrational contributions. In the first step of the calculations, statistical thermodynamical calculations were performed using a rigid rotor/harmonic oscillator model. The calculations were performed at 130 K, i.e. at the midpoint of the temperature interval used during the experimental study. Subsequently, for each species, the solvation Gibbs energies in LKr were estimated at 6 different temperatures, varying from 94 to 154 K, at a pressure of 28 bar and the enthalpy of solvation $\Delta_{sol}H$ was extracted using the expression $\Delta_{sol}H = \Delta_{sol}G + T\Delta_{sol}S$ with the entropy of solvation $\Delta_{sol}S = -(\partial \Delta_{sol}G/\partial T)_p$. The values for the vapor phase complexation enthalpies and the corresponding values for the solutions studied are collected in Table 9.

### 3.3. Vibrational spectra

The vibrational spectra of the trifluorohalomethanes $CF_3Cl$, $CF_3Br$, $CF_3I$ [20-23,46-49] and of ethyne and propyne [29,30] dissolved in liquid noble gases have been reported before. The characteristic frequencies for 2-butyne in LKr and their assignments, based on literature data for the vapor and liquid phases [50,51] and on the harmonic vibrational frequencies derived at the MP2/aug-cc-pVD(T)Z levels, are summarized in Table S10 of the ESI. The results show that for almost all modes, a good agreement is found between theory and experiment. The most significant deviation is observed for the symmetric C-C≡C-C stretching mode $\nu_{16}$ ($E_{1g}$). This mode appears in the Raman spectra near 370 $cm^{-1}$, while the calculated values for the aug-cc-pVDZ and aug-cc-pVTZ basis sets are 198.7 and 354.6 $cm^{-1}$, respectively. The rather large deviation between theory and experiment observed for aug-cc-pVDZ tend to suggest that even for Dunning type basis sets significant basis set incompleteness errors [52-55] can

appear and that the appearance of these errors thus is not limited to Pople type basis sets. These errors, obviously, are corrected by expanding the basis set.

To characterize the different complexes formed in the cryosolutions, in this study the infrared and Raman spectra of solutions in LKr, containing different concentrations of halogen donors and acceptors, were investigated at temperatures between 120 K and 140 K. For the infrared studies, the mole fractions of the trifluorohalomethanes and the different alkynes ethyne, propyne and 2-butyne were varied between $9.4 \times 10^{-5}$ and $2.5 \times 10^{-2}$, between $1.9 \times 10^{-4}$ and $2.8 \times 10^{-3}$, between $9.4 \times 10^{-5}$ and $1.9 \times 10^{-3}$ and between $9.4 \times 10^{-5}$ and $1.9 \times 10^{-3}$, respectively. The corresponding mole fractions used in the Raman were varied between $7.1 \times 10^{-3}$ and $1.3 \times 10^{-2}$, between $4.7 \times 10^{-3}$ and $7.1 \times 10^{-3}$, between $3.8 \times 10^{-3}$ and $5.6 \times 10^{-3}$ and between $3.8 \times 10^{-3}$ and $4.7 \times 10^{-3}$. Even for a large excess of the halogen donor, for none of the alkynes studies, experimental evidence illustrating the existence of C-Cl$\cdots\pi$ bonded complexes was observed. For the solutions containing ethyne, weak spectral features illustrating the occurrence of halogen bonded complexes were observed for the solutions containing $CF_3I$ only. The frequencies, their assignment and complexation shifts observed for the complexes of ethyne, propyne and 2-butyne are collected in Table 10, Tables 11 and 12, and Tables 13 and 14, respectively.

From the calculated harmonic vibrational frequencies collected in Tables 5, 6 and 7, it can be seen that upon complexation with the carbon-carbon triple bond, significant complexation shifts are predicted for the symmetric and antisymmetric $CF_3$ stretching modes in the halogen donors. The corresponding spectral regions obtained by studying the infrared spectra of solutions in LKr containing mixtures of the respective alkynes and $CF_3I$ have been summarized in Fig. 3. The spectra obtained for the different alkynes ethyne, propyne and 2-butyne have been separated in panels A, B, and C. For each panel, the spectrum for the mixed solution, recorded at 120K, is given in the top trace, while the corresponding spectra of the monomers are given in the middle and bottom trace. Bands assigned to the 1:1 halogen bonded complexes are marked with an asterisk. Because of the large infrared intensities of the $CF_3$ stretching modes involved, during all studies, low concentrations of $CF_3X$ had to be used to avoid full absorption in this region. As a consequence, complexation was forced by using a large excess of the alkyne studied, typical mole fractions being in the order of $8.0 \times 10^{-5}$ for the halogen donor and $2.0 \times 10^{-3}$ for the alkyne.

For the solutions containing ethyne, a weak band assigned to the antisymmetric $\nu_4$ stretching modes in the complex with $CF_3I$ was observed at 1168.5 $cm^{-1}$. The experimental shift of -6.8 $cm^{-1}$ is in excellent agreement with the predicted value of -7.1 $cm^{-1}$. No complex band was observed for the monomer symmetric stretching mode $\nu_1$.

For the solutions containing propyne and 2-butyne, additional bands assigned to the antisymmetric and symmetric stretching modes $\nu_4$ and $\nu_1$ in the complex with $CF_3I$ were observed at

1165.4 and 1072.6 $cm^{-1}$, and at 1163.0 and 1073.6 $cm^{-1}$, respectively. The experimental complexation shifts, -10.0 and 7.1 $cm^{-1}$ for propyne and -12.4 and 8.1 $cm^{-1}$ for 2-butyne, again compare favorably with the predicted values of -9.6 and 6.1 $cm^{-1}$ and of -12.0 and 7.1 $cm^{-1}$. Apart from the bands reported above, weak spectral features due to the $CF_3$ stretching modes in the $^{13}C$ isotopomers are also observed near 1132.8 and 1043.6 $cm^{-1}$, and near 1130.5 and 1044.2 $cm^{-1}$, respectively.

The spectra collected in the panels of Fig. 3 have been obtained by using similar concentrations of the halogen donors and acceptors and, consequently, give direct insight into the degree of complexation, and the chemical equilibria involved. Inspection of the relative intensities in the spectra obtained for the different solutions therefore suggests that the interactions with 2-butyne are significantly stronger than those with propyne, and that ethyne forms the weakest halogen bond in the series of Lewis bases presented. A similar conclusion, albeit indirectly, can be obtained from the changes in complexation shifts showing a significant increases from ethyne to propyne and from propyne to 2-butyne.

Analyses similar to those reported above have also been performed for the solutions containing $CF_3Br$. The corresponding spectral regions obtained for solutions containing mixtures of propyne and 2-butyne with $CF_3Br$, are summarized in Fig. S1 of the supporting information. The characteristic frequencies for the monomers and the complexes, and the complexation shifts observed are included in Tables 12 and 14. The analysis of the relative intensities, the monomer concentrations used and the trends observed for the complexation shifts show that for both propyne and 2-butyne, the complexes with $CF_3I$ are significantly stronger than those with $CF_3Br$. This result, obviously, is in line with the results derived from the ab initio calculations.

Apart from the shifts observed for the $CF_3$ stretching modes, significant complexations shifts have also been predicted for the C-X stretching modes. These modes are characterized by a very low infrared intensity in the monomers and, consequently, are preferentially studied using Raman spectroscopy [20-23]. The characteristic spectral regions obtained by studying the Raman spectra of solutions in LKr, at 120 K, containing mixtures of $CF_3I$ with ethyne, propyne and 2-butyne, are shown in Figs. 4A, 4B and 4C, respectively. As before, the spectra of the mixed solutions are given in the top trace, while the spectra of the monomers are given in the middle and bottom trace. The new bands assigned to the halogen bonded complexes again are marked with an asterisk. The spectra were recorded using an approximate mole fraction of $7.0 \times 10^{-3}$ for $CF_3I$ and of $5.0 \times 10^{-3}$ for the different alkynes.

In addition to the 288.6 $cm^{-1}$ monomer band involved, for the mixtures of $CF_3I$ and ethyne, no new band indicating complexation with ethyne was found for the C-I stretching mode $\nu_3$. In contrast, for both propyne and 2-butyne, additional bands illustrating the occurrence of halogen bonded species were observed near 285.9 and 285.2 $cm^{-1}$. The experimental red shifts observed, -2.7 $cm^{-1}$ for propyne and -3.4 $cm^{-1}$ for 2-butyne, compare favorably with the calculated shifts of -3.3 and -5.1 $cm^{-1}$. Moreover, the

changes in the complexation shifts support the general ideas about the differences in relative stability discussed above. The experimental red shifts are also in line with the values of -2.6 and -3.6, reported for ethene·$CF_3I$ and propene·$CF_3I$, respectively.

The data reported above clearly shows that new bands due to the formation of halogen bonded complexes can readily be observed for a variety of modes localized in the halogen donor molecules. Inspection of the calculated frequencies in Tables 5, 6 and 7 shows that also for modes localized in the acceptor molecules including, for example, the C≡C stretching vibrations, changes in vibrational frequencies and intensities are predicted.

In Fig. 5, the spectral regions for the various C≡C stretching modes, obtained by studying the infrared and Raman spectra of mixed solutions in LKr containing $CF_3I$ and ethyne, propyne or 2-butyne, and of solutions containing only monomers, are compared. The spectral data derived from the Raman experiments with ethyne, propyne and 2-butyne are given in panels A, C and E, respectively. The corresponding infrared data are given in panels B, D, and F. For the panels A, B, C and E, traces *a, b* and *c*, refer to the spectra obtained for the mixed solution, for the monomer alkyne and for monomer $CF_3I$, respectively. For panels D and F, traces *a*, *b* and *c* refer to the spectra obtained for the mixed solution, for monomer propyne or 2-butyne and for monomer $CF_3I$, while trace *d* gives the spectrum of the isolated complex obtained by subtracting the spectrum of the mixed solution with the rescaled monomer spectra of 2-butyne and $CF_3I$.

The Raman spectral data summarized in panels A, C and E, clearly shows that apart from the monomer transitions at 1970.1, 2136.7 and 2247.8 $cm^{-1}$, new bands due to the stretching modes in the complexes can be observed near 1966.5, 2130.0 and 2237.6 $cm^{-1}$, respectively. The additional weak features observed at 2129.6 $cm^{-1}$ in trace *b* and at 2123.0 and 2128.3 $cm^{-1}$ in trace *c* of panel C are due to a, yet unassigned, combination band or overtone in propyne, and to combination bands involving the $CF_3$ stretching modes in the halogen donor [20-23,46-49]. These bands, at first glance, have no direct counterpart in the spectra of the complexes. The intense feature at 2229.2 $cm^{-1}$, marked with a circle (°) in the spectra of the mixed solutions containing 2-butyne and $CF_3I$, will be discussed in more detail below.

The Raman data for propyne can directly be compared with the infrared data in panel D showing the appearance of monomer and complex bands at exactly the same frequencies as those observed in the Raman spectra. The analysis of the infrared data obtained for ethyne and 2-butyne is less straightforward as the C≡C stretching mode in these species is infrared forbidden in the monomer and gains a relatively small, induced infrared intensity in the complex.

Inspection of the data in panel B shows that in the infrared spectra of the solutions containing mixtures of ethyne and $CF_3I$, a weak feature due to the induced C≡C stretching mode in the complex can

be observed, near 1966.5 $cm^{-1}$, i.e. at a frequency closely resembling that deduced from the Raman studies. The appearance of a weak feature due to the induced C≡C stretching vibration is in line with the predicted infrared intensities in Table S3 showing a weak infrared intensity of some 1.7 km $mol^{-1}$ for the stretching mode in the complex with $CF_3I$. The results are also in line with previous experimental observations showing the appearance of induced C≡C stretching modes while forming complexes of ethyne with Lewis bases such as HCl and $BF_3$ [29,30] and the appearance of induced C=C stretching modes while forming complexes of ethene with, amongst others, $CF_3I$ [21].

The calculated infrared intensities in Table S9 show that also for 2-butyne, the complexation with $CF_3I$ leads to an induced infrared intensity of some 4.7 km $mol^{-1}$for the C≡C stretching mode. Unfortunately, the appearance of relatively strong absorption features related to the $\nu_4 + \nu_5 + 2\nu_6$ / $\nu_1 + \nu_4$ / $\nu_4 + 2\nu_5$ / $\nu_4 + 4\nu_6$ resonances in monomer $CF_3I$ [22,47] and in the complex with 2-butyne, hampered the observation of the spectral features related to the induced C≡C stretching mode in the complexes with $CF_3I$. However, it is worth noting that additional information on the induced C≡C stretching modes in complexes with 2-butyne, and their relationship to the induced stretching modes appearing in the complexes with ethyne might be obtained by studying the complexes of both Lewis bases with classical Lewis acids such as $BF_3$ or HCl, or, eventually, with other hydrogen donating molecules such as fluoroform, $CHF_3$ [39,57], and halothane, $CHBrClCF_3$. [32,58] Such investigations were considered as being beyond the scope of the current study and were not pursued here.

It was noted above that, apart from the bands assigned to the monomers and to the 1:1 complexes, an additional spectral feature at 2229.2 $cm^{-1}$ is observed in the Raman spectra of the mixed solutions containing 2-butyne and $CF_3I$. This band, marked with a circle (°) in panel E of Fig. 5, is only observed at lower temperatures and at higher concentrations of $CF_3I$, in agreement with similar observations made for mixed solutions containing dimethyl sulfide and $CF_3I$, and dimethyl ether and $CF_3Br$ [20,22] and is assigned to the C≡C stretching mode in a 2:1 complex consisting of one 2-butyne molecule and two $CF_3I$ moieties. The assignment of the 2229.2 $cm^{-1}$ band to a 2:1 complex is confirmed by a concentration study (vide infra) and is further supported by the results from the ab initio calculations reported above, and by additional experimental evidence for the formation of such a complex derived from the $2\nu_8$ and $\nu_2+\nu_4$ spectral regions of 2-butyne and of $CF_3I$, respectively. These spectral regions are presented in Figure 6. The characteristic frequencies derived from the infrared and Raman data, and the corresponding data derived from the ab initio calculations supporting their assignment are given in Table 8.

### 3.4. Stoichiometry

The stoichiometry of the complexes observed was established from isothermal spectra in which the concentrations of the solutes were systematically varied, using a procedure similar to that described

before [20-23] The analysis is based upon the fact that the integrated intensity of a complex band under study $I_{A_mB_n}$ is linearly related to the product of the $m^{th}$ power of the monomer band area $I_A$ and the $n^{th}$ power of the monomer band area $I_B$. By plotting the complex band area $I_{complex}$ versus the products of the monomer band areas $(I_A)^x(I_B)^y$ for various integer values of $x$ and $y$ the stoichiometry of the complex can be determined.

Typical values for the goodness of fit parameter $\chi^2$ for the mixed solutions containing $CF_3I$ and 2-butyne, obtained by using the integrated band areas for the 1163.0 $cm^{-1}$ complex band and the 740.7 and 2867.7 $cm^{-1}$ monomer bands, and by assuming a proposed 1:1, 2:1 and 1:2 stoichiometry are 0.009, 1.682 and 1.387. These values clearly confirm the above assignments to complexes with a 1:1 stoichiometry. The typical values obtained for the 1898.8 $cm^{-1}$ complex band, being 0.0234, 0.0003 and 0.0020, also support the formation of a 2:1 halogen bonded complex, consisting of two $CF_3I$ moieties and one 2-butyne molecule.

### 3.5. Relative Stability

The standard complexation enthalpies for the 1:1 and 2:1 complexes were derived from a temperature study of different solutions using the Van't Hoff relation. This establishes a linear relation, with a slope related to $-[\Delta H°(\mathrm{LKr}) + (m+n-1)Rb]/R$, between the inverse temperature and the logarithm of the intensity product $I_{complex}/\left(I_{CF_3X} \times I_{alkyne}\right)$ in which $I_{CF_3X}$, $I_{alkyne}$ and $I_{complex}$ are the intensities of a band of the monomers and of the complex. The factor $b$ in the slope of this linear relation is a correction factor to account for the changes in solvent density upon temperature variation [59].

Typical Van't Hoff plots obtained for the different complexes and the resulting linear regression lines are shown in Fig. 7. The average complexation enthalpies for the 1:1 complexes, obtained by analyzing and averaging out the data for a series of solutions and by correcting the slopes of the different regression lines for density variations in the temperature intervals used,[29] are -5.9(3) kJ $mol^{-1}$ for $CF_3I$•ethyne, -5.6(3) kJ $mol^{-1}$ for $CF_3Br$•propyne, -8.1(2) kJ $mol^{-1}$ for $CF_3I$•propyne, -7.3(2) kJ $mol^{-1}$ for $CF_3Br$•2-butyne and -10.9(2) kJ $mol^{-1}$ for $CF_3I$•2-butyne. The Van 't Hoff plot for the 2:1 complex formed between 2-butyne and $CF_3I$ is also shown in Figure 7. The cumulative complexation enthalpy, obtained by assuming the complexation equilibrium 2-butyne + $CF_3I$ ⇌ 2-butyne•$(CF_3I)_2$ equals -20.9(7) kJ $mol^{-1}$.

Comparison of the experimental and predicted values for the complexation enthalpies show that for the different alkynes and trifluorohalomethanes studied, a good correlation is found between experiment and theory, and that the general trends predicted by the ab initio calculations are neatly reproduced by the experiments. In general, however, the predicted values derived from the MP2/aug-cc-pVTZ(-PP) energies are overestimated by approximately 30%.

To further rationalize the trends observed, the calculated and experimental complexation enthalpies obtained for the various alkynes, and the corresponding results obtained for ethene and propene [21], and for benzene and toluene [27] are shown in Fig.8. The regression lines lead to a scale factor of 0.946(71) for the alkenes, 0.695(9) for the alkynes and 0.568(42) for the aromatic model compounds, respectively. These results tend to suggest that, for the interactions with alkenes, the predicted complexation enthalpies neatly reproduce the experimental values, with the differences between experiment and theory being in the order of a mere 5 to 10%. In contrast, for the alkynes and the aromatic model systems, the calculated values tend to be seriously overestimated, by approximately 30 and 45%, respectively. Although the overestimation of the MP2 method for aromatic systems has been observed before [60,61], so far no insight explaining these observations have been put forward.

## 4. Conclusions

By analyzing the infrared and Raman spectra of mixed and monomer solutions in liquid krypton, over a temperature range between 120 K to 140 K, experimental evidence for several C-X$\cdots\pi$ halogen bonded complexes was obtained. The experimental complexation enthalpies derived from the temperature studies are -5.9(3) kJ mol$^{-1}$ for $CF_3I$•ethyne, -5.6(3) kJ mol$^{-1}$ for $CF_3Br$•propyne, -8.1(2) kJ mol$^{-1}$ for $CF_3I$•propyne, -7.3(2) kJ mol$^{-1}$ for $CF_3Br$•2-butyne and -10.9(2) kJ mol$^{-1}$ for $CF_3I$•2-butyne, and show for the series of Lewis bases studied 2-butyne forms the strongest halogen bonds, while ethyne gives rise to the weakest complexes. Infrared and Raman experiments also revealed the existence of a 2:1 complex with 2 molecules $CF_3I$ bonded to a single 2-butyne molecule. The experimental complexation enthalpy for this complex is -20.9(7) kJ mol$^{-1}$.

Comparison of the results obtained in this study with previous studies on the halogen bonding of $CF_3X$ (X = Br, I) with ethene and propene [21] shows that the complex with ethyne is significantly weaker than the corresponding complex with ethene, while the complexes with propyne and propene have a similar stability.

## Acknowledgements

The FWO-Vlaanderen is thanked for their assistance towards the purchase of spectroscopic equipment used in this study. The authors thank the Flemish Community for financial support through the Special Research Fund (BOF). Financial support through the 'Impulsfinanciering voor Grote Apparatuur' and 'Hercules Foundation' allowing the purchase of the CalcUA supercomputing clusters is acknowledged.

**References**


[1] G. Mínguez Espallargas, F. Zordan, L. Arroyo Marín, H. Adams, K. Shankland, J. van de Streek and L. Brammer, Chemistry – A European Journal 15 (2009) 7554-7568.

[2] A. Priimagi, M. Saccone, G. Cavallo, A. Shishido, T. Pilati, P. Metrangolo and G. Resnati, Advanced Materials 24 (2012) OP345-OP352.

[3] J. Marti-Rujas, L. Colombo, J. Lu, A. Dey, G. Terraneo, P. Metrangolo, T. Pilati and G. Resnati, Chemical Communications 48 (2012) 8207-8209.

[4] L. Meazza, J. A. Foster, K. Fucke, P. Metrangolo, G. Resnati and J. W. Steed, Nature Chemistry 5 (2012) 42-47.

[5] R. Wilcken, M. O. Zimmermann, A. Lange, A. C. Joerger and F. M. Boeckler, Journal of Medicinal Chemistry 56 (2013) 1363-1388.

[6] Z. Xu, Z. Liu, T. Chen, T. Chen, Z. Wang, G. Tian, J. Shi, X. Wang, Y. Lu, X. Yan, G. Wang, H. Jiang, K. Chen, S. Wang, Y. Xu, J. Shen and W. Zhu, Journal of Medicinal Chemistry 54 (2011) 5607-5611.

[7] A. V. Jentzsch, D. Emery, J. Mareda, S. K. Nayak, P. Metrangolo, G. Resnati, N. Sakai and S. Matile, Nature Communication 3 (2012) 905.

[8] N. F. Valadares, L. B. Salum, I. Polikarpov, A. D. Andricopulo and R. C. Garratt, Journal of Chemical Information and Modeling 49 (2009) 2606-2616.

[9] Y. Lu, H. Li, X. Zhu, H. Liu and W. Zhu, Journal of Molecular Modeling 8 (2012) 3311-3320.

[10] A. J. Parker, J. Stewart, K. J. Donald and C. A. Parish, Journal of the American Chemical Society 134 (2012) 5165-5172.

[11] P. Metrangolo, G. Resnati, T. Pilati, R. Liantonio and F. Meyer, Journal of Polymer Science Part A: Polymer Chemistry 45 (2007) 1-15.

[12] P. Politzer, P. Lane, M. Concha, Y. Ma and J. Murray, Journal of Molecular Modeling 13 (2007) 305-311.

[13] P. Metrangolo and G. Resnati, Halogen Bonding: Fundamentals and Applications, Springer, Berlin, 2008.

[14] K. Rissanen, CrystEngComm 10 (2008) 1107-1113.

[15] M. Erdelyi, Chemical Society Reviews 41 (2012) 3547-3557.

[16] P. Politzer, K. E. Riley, F. A. Bulat and J. S. Murray, Computational and Theoretical Chemistry 998 (2012) 2-8.

[17] S. L. Stephens, W. Mizukami, D. P. Tew, N. R. Walker and A. C. Legon, Journal of Molecular Spectroscopy (2012) 47-53.

[18] S. L. Stephens, N. R. Walker and A. C. Legon, Journal of Chemical Physics 135 (2011) 224309-224317.

[19] G. Feng, L. Evangelisti, N. Gasparini and W. Caminati, Chemistry - A European Journal 18 (2012) 1364-1368.

[20] D. Hauchecorne, A. Moiana, B. J. van der Veken and W. A. Herrebout, Physical Chemistry Chemical Physics 13 (2011) 10204-10213.

[21] D. Hauchecorne, N. Nagels, B. J. van der Veken and W. A. Herrebout, Physical Chemistry Chemical Physics 14 (2012) 681-690.

[22] D. Hauchecorne, R. Szostak, W. A. Herrebout and B. J. van der Veken, ChemPhysChem 10 (2009) 2105-2115.

[23] D. Hauchecorne, B. J. van der Veken, A. Moiana and W. A. Herrebout, Chemical Physics 374 (2010) 30-36.

[24] L. J. Liu, W. A. Baase and B. W. Matthews, Journal of Molecular Biology 385 (2009) 595-605.

[25] H. Matter, M. Nazare, S. Gussregen, D. W. Will, H. Schreuder, A. Bauer, M. Urmann, K. Ritter, M. Wagner and V. Wehner, Angewandte Chemie-International Edition 48 (2009) 2911-2916.

[26] L. Xu, P. Sang, J. W. Zou, M. B. Xu, X. M. Li and Q. S. Yu, Chemical Physics Letters 509 (2011) 175-180.

[27] N. Nagels, D. Hauchecorne and W. A. Herrebout, Molecules, submitted for publication.

[28] O. V. Shishkin, R. I. Zubatyuk, V. V. Dyakonenko, C. Lepetit and R. Chauvin, Physical Chemistry Chemical Physics 13 (2011) 6837-6848.

[29] W. A. Herrebout, J. Lundell and B. J. van der Veken, Journal of Physical Chemistry A 103 (1999) 7639-7645.

[30] W. A. Herrebout, J. Lundell and B. J. van der Veken, Journal of Molecular Structure 480-481 (1999) 489-493.

[31] G. P. Everaert, W. A. Herrebout, B. J. van der Veken, J. Lundell and M. Räsänen, Chemistry – A European Journal 4 (1998) 321-327.

[32] B. Michielsen, W. A. Herrebout and B. J. van der Veken, ChemPhysChem 8 (2007) 1188-1198.

[33] A. A. Stolov, W. A. Herrebout and B. J. van der Veken, Journal of the American Chemical Society 120 (1998) 7310-7319.

[34] J. J. J. Dom, B. Michielsen, B. U. W. Maes, W. A. Herrebout and B. J. van der Veken, Chemical Physics Letters 469 (2009) 85-89.

[35] W. A. Herrebout, N. Nagels and B. J. van der Veken, ChemPhysChem 10 (2009) 3054-3060.

[36] M. J. Frisch, G. W. Trucks, H. B. Schlegel, G. E. Scuseria, M. A. Robb, J. R. Cheeseman, G. Scalmani, V. Barone, B. Mennucci, G. A. Petersson, H. Nakatsuji, M. Caricato, X. Li, H. P. Hratchian, A. F. Izmaylov, J. Bloino, G. Zheng, J. L. Sonnenberg, M. Hada, M. Ehara, K. Toyota, R. Fukuda, J. Hasegawa, M. Ishida, T. Nakajima, Y. Honda, O. Kitao, H. Nakai, T. Vreven, J. A. Montgomery, J. E. Peralta, F. Ogliaro, M. Bearpark, J. J. Heyd, E. Brothers, K. N. Kudin, V. N. Staroverov, R. Kobayashi, J. Normand, K. Raghavachari, A. Rendell, J. C. Burant, S. S. Iyengar, J. Tomasi, M. Cossi, N. Rega, J. M.

Millam, M. Klene, J. E. Knox, J. B. Cross, V. Bakken, C. Adamo, J. Jaramillo, R. Gomperts, R. E. Stratmann, O. Yazyev, A. J. Austin, R. Cammi, C. Pomelli, J. W. Ochterski, R. L. Martin, K. Morokuma, V. G. Zakrzewski, G. A. Voth, P. Salvador, J. J. Dannenberg, S. Dapprich, A. D. Daniels, Farkas, J. B. Foresman, J. V. Ortiz, J. Cioslowski and D. J. Fox in Gaussian 09, Revision B.01, Wallingford CT, 2009.

[37] B. Pinter, N. Nagels, W. A. Herrebout and F. De Proft, Chemistry – A European Journal 19 (2013) 519-530.

[38] R. M. Levy and E. Gallicchio, Annual Review of Physical Chemistry 49 (1998) 531-567.

[39] S. N. Delanoye, W. A. Herrebout and B. J. van der Veken, The Journal of Physical Chemistry A (2005) 9836-9843.

[40] W. Vanspeybrouck, W. A. Herrebout, B. J. van der Veken, J. Lundell and R. N. Perutz, The Journal of Physical Chemistry B 107 (2003) 13855-13861.

[41] J. H. Knox, Molecular thermodynamics: An introduction to statistical mechanics for chemists, Wiley-Interscience, Londen, 1971.

[42] D. A. McQuarrie and J. D. Simon, Physical Chemistry: A molecular approach, University Science Books, California, 1997.

[43] T. Clark, M. Hennemann, J. Murray and P. Politzer, Journal of Molecular Modeling 13 (2007) 291-296.

[44] N. A. Young, Coordination Chemistry Reviews 257 (2013) 956-1010.

[45] C. M. Breneman and K. B. Wiberg, Journal of Computational Chemistry 11 (1990) 361-373.

[46] A. Baldacci, A. Passerini and S. Ghersetti, Journal of Molecular Spectroscopy 91 (1982) 103-115.

[47] M. O. Bulanin, L. A. Zhigula, T. D. Kolomiitsova and D. N. Shchelpkin, Optics and Spectroscopy 56 (1984) 663–669.

[48] H. Bürger, K. Burczyk, R. Grassow and A. Ruoff, Journal of Molecular Spectroscopy 93 (1982) 55-73.

[49] K. Scanlon, I. Suzuki and J. Overend, The Journal of Chemical Physics 74 (1981) 3735-3744.

[50] I. M. Mills and H. W. Thompson, Proceedings of the Royal Society of London. Series A. Mathematical and Physical Sciences 228 (1955) 287-297.

[51] L. M. Sverdlov, M. A. Kovner and E. P. Krainov, Vibrational Spectra of Polyatomic Molecules, Halsted, New York, 1973.

[52] D. Asturiol, M. Duran and P. Salvador, Journal of Chemical Physics 128 (2008) 144108-144113.

[53] R. M. Balabin, Journal of Chemical Physics 132 (2010) 231101-231105.

[54] R. M. Balabin, Structural Chemistry 22 (2011) 1047-1051.

[55] N. C. Handy, P. E. Maslen, R. D. Amos, J. S. Andrews, C. W. Murray and G. J. Laming, Chemical Physics Letters 197 (1992) 506-515.

[56] D. Moran, A. C. Simmonett, F. E. Leach, W. D. Allen, P. v. R. Schleyer and H. F. Schaefer, Journal of the American Chemical Society 128 (2006) 9342-9343.

[57] W. A. Herrebout, S. M. Melikova, S. N. Delanoye, K. S. Rutkowski, D. N. Shchepkin and B. J. van der Veken, The Journal of Physical Chemistry A 109 (2005) 3038-3044.

[58] B. Michielsen, J. J. J. Dom, B. J. van der Veken, S. Hesse, M. A. Suhm and W. A. Herrebout, Physical Chemistry Chemical Physics 14 (2012) 6469-6478.

[59] B. J. Van der Veken, The Journal of Physical Chemistry 100 (1996) 17436-17438.

[60] B. Michielsen, J. J. J. Dom, B. J. van der Veken, S. Hesse, Z. Xue, M. A. Suhm and W. A. Herrebout, Physical Chemistry Chemical Physics 12 (2010) 14034-14044.

[61] J. J. J. Dom, B. J. van der Veken, B. Michielsen, S. Jacobs, Z. Xue, S. Hesse, H.-M. Loritz, M. A. Suhm, W. Herrebout, Physical Chemistry Chemical Physics 13 (2011) 14142-14152.

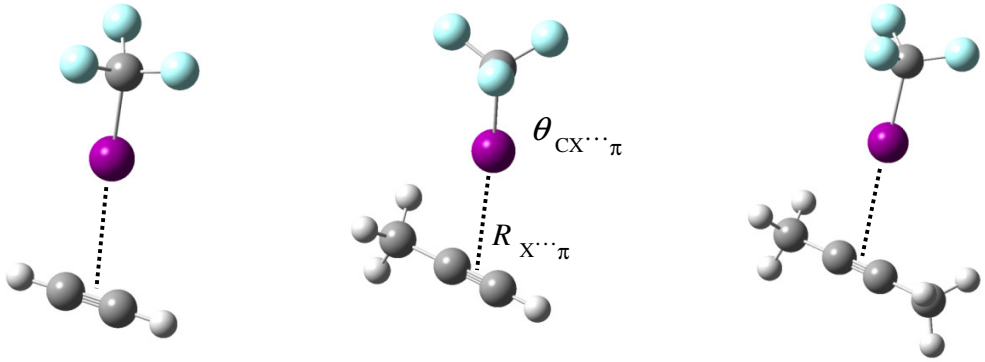


**Fig. 1.**

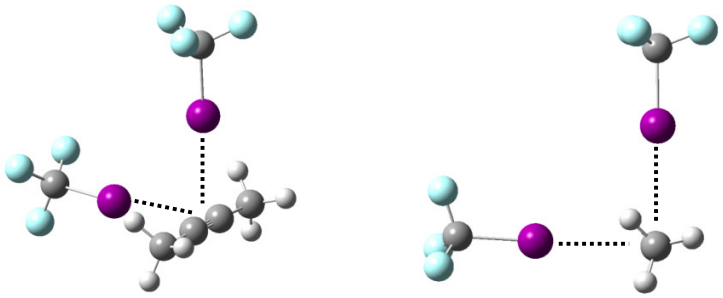

**Fig. 2**

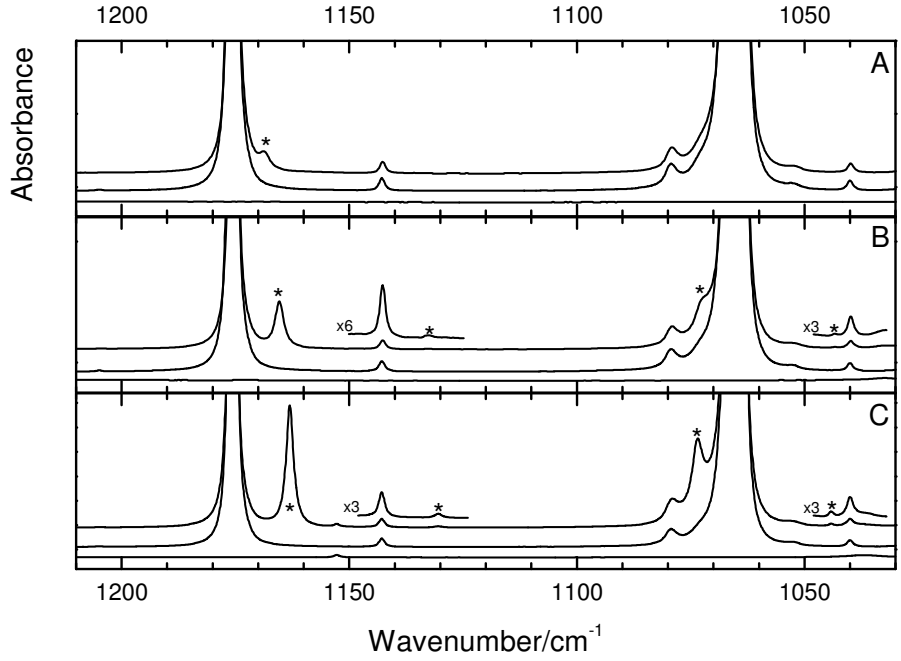
1200
1150
1100
1050
Absorbance
A
B
C
x6
x3
x3
x3
Wavenumber/cm-1

**Fig. 3**

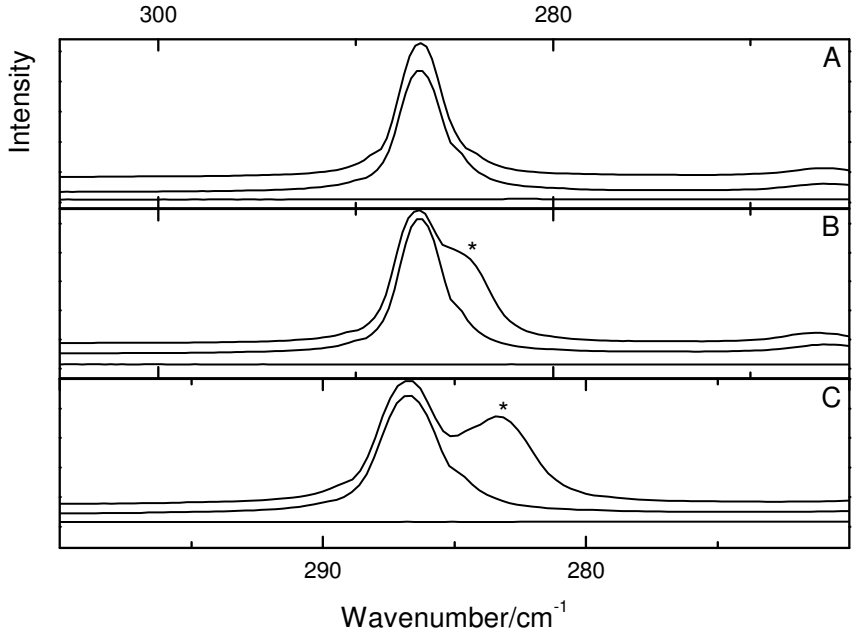
300
280
Intensity
A
B
C
290
280
Wavenumber/cm-1

**Fig. 4**

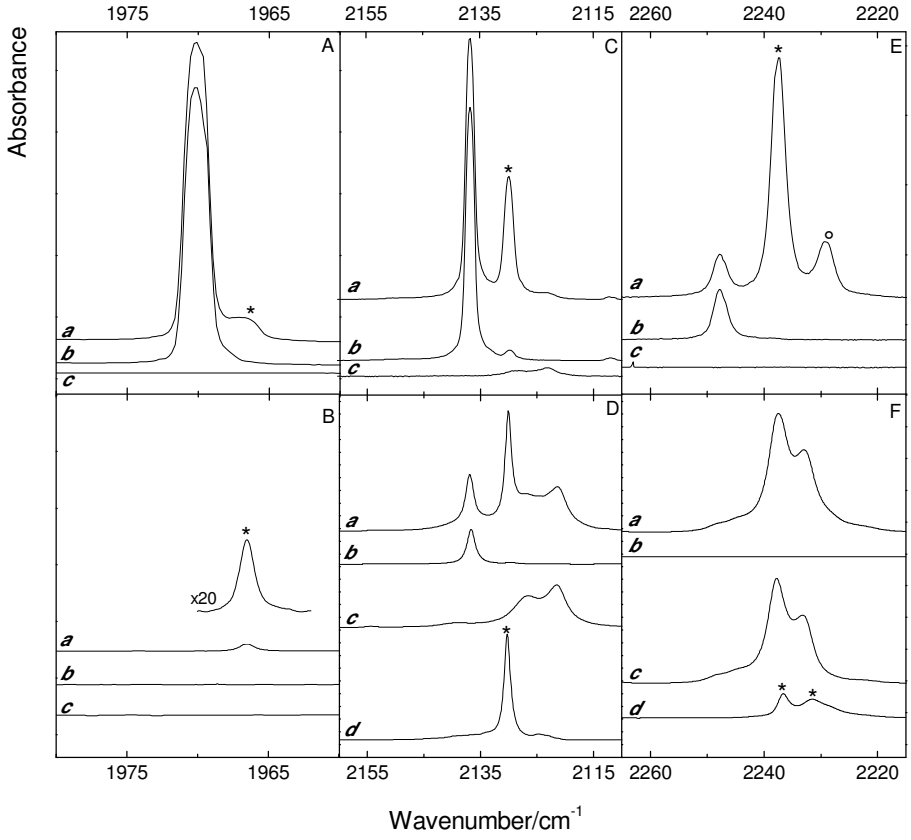
1975
1965
2155
2135
2115
2260
2240
2220
A
C
E
B
D
F
Absorbance
a
b
c
d
*
°
x20
Wavenumber/cm-1

**Fig. 5**

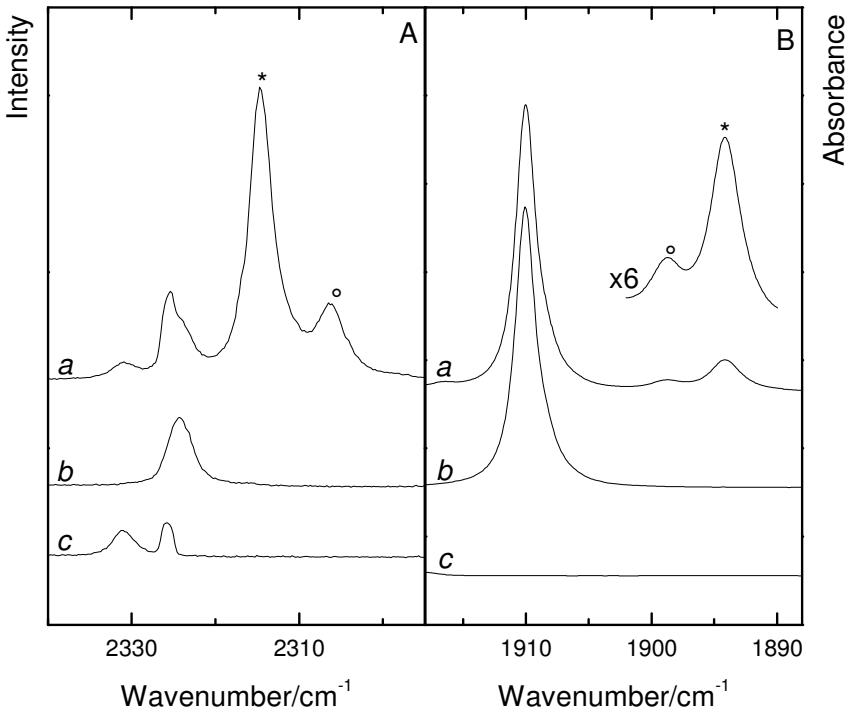
Intensity
A
B
Absorbance
*
°
x6
a
b
c
2330
2310
1910
1900
1890
Wavenumber/cm-1
Wavenumber/cm-1

**Fig. 6**

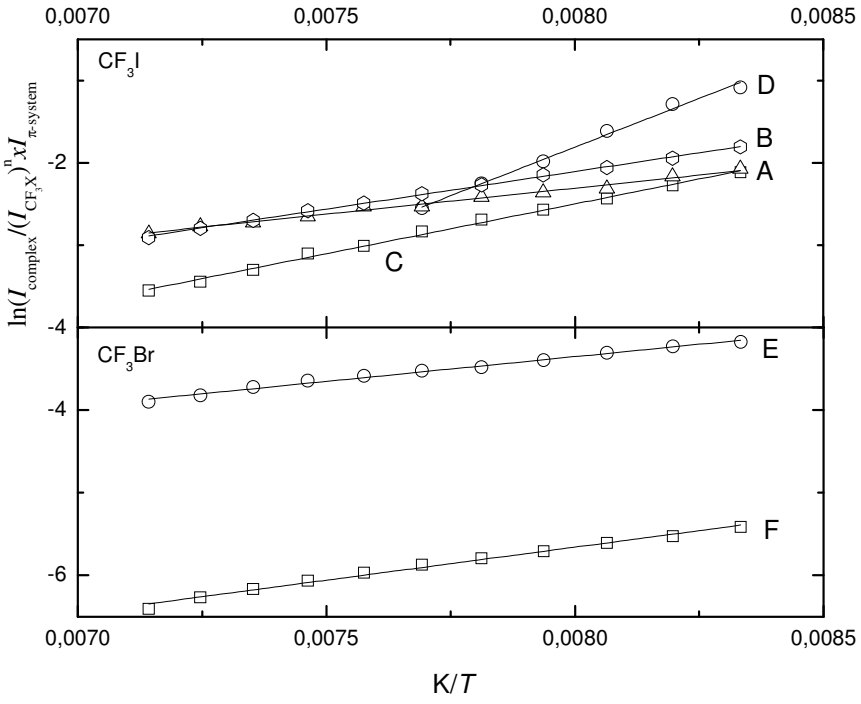
0,0070
0,0075
0,0080
0,0085
CF3I
CF3Br
D
B
A
C
E
F
-2
-4
-4
-6
ln(Icomplex/(ICF3X)nxIπ-system
K/T

**Fig. 7**

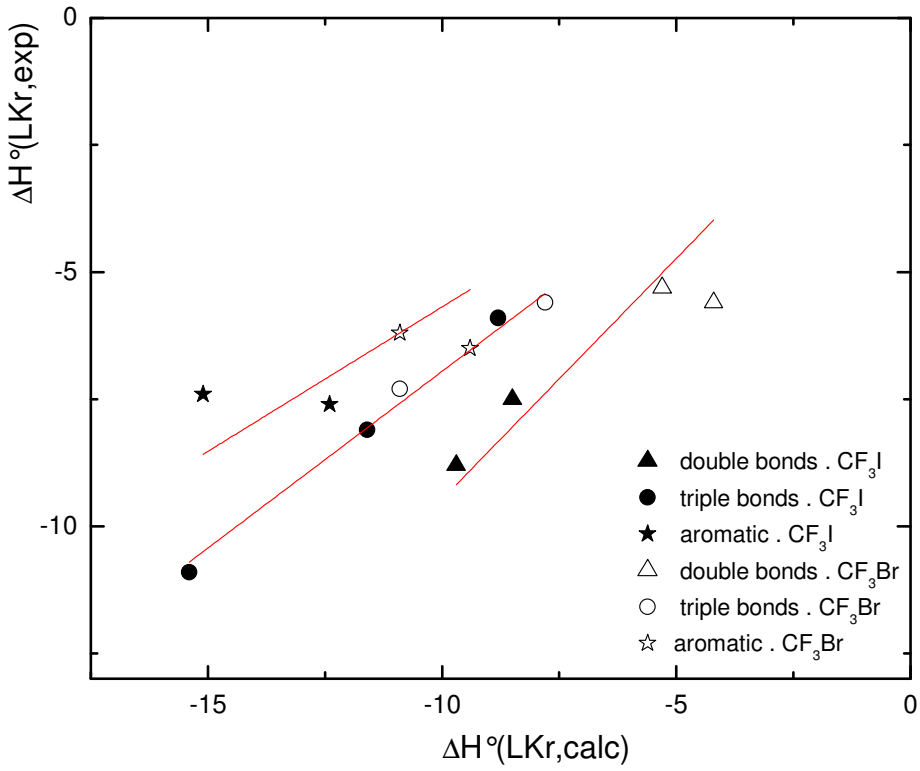
0
-5
-10
-15
-10
-5
0
ΔH°(LKr,exp)
ΔH°(LKr,calc)
double bonds . CF3I
triple bonds . CF3I
aromatic . CF3I
double bonds . CF3Br
triple bonds . CF3Br
aromatic . CF3Br

**Fig. 8**

**Figure Captions**

Fig. 1. MP2/aug-cc-pVDZ(-PP) equilibrium geometries for the complexes of $CF_3X$ (X = Cl, Br and I) with ethyne (left), propyne (middle) and 2-butyne (right).

Fig. 2. MP2/aug-cc-pVDZ-PP equilibrium geometry for the 2:1 complex of $CF_3I$ with 2-butyne.

Fig. 3. Infrared spectra in the 1210-1030 $cm^{-1}$ spectral region for solutions in liquid krypton, at 120 K, containing mixtures of $CF_3I$ with ethyne (panel A), propyne (panel B) and 2-butyne (panel C). In each panel the top trace represents the mixed solution, while the middle and bottom traces show solutions containing only $CF_3I$ and ethyne, propyne or 2-butyne, respectively. New bands due to the 1:1 complexes are marked with an asterisk (*).

Fig. 4. Raman spectra in the 305-265 $cm^{-1}$ spectral region for solutions in liquid krypton, at 120 K, containing mixtures of $CF_3I$ with ethyne (panel A), propyne (panel B) and 2-butyne (panel C). In each panel the top trace represents the mixed solution, while the middle and bottom traces show the solution containing only $CF_3I$ and ethyne, propyne or 2-butyne, respectively. New bands due to the 1:1 complexes are marked with an asterisk (*).

Fig. 5. Raman spectra (panels A, C and E) and infrared spectra (panels B, D and F) of the $\nu_{C\equiv C}$ spectral region for solutions of mixtures of $CF_3I$ with ethyne (panels A and B), propyne (panels C and D) and 2-butyne (panels E and F) dissolved in liquid krypton at 120K. In each panel, trace *a* represents the mixed solution, while traces *b* and *c* show the solution containing only $CF_3I$ or ethyne, propyne or 2-butyne. Trace *d* in panels D and F is obtained by subtracting traces *b* and *c* from trace *a*. New bands due to the 1:1 complex appearing in the spectrum of the mixture are marked with an asterisk (*). Bands marked with a circle (o) are assigned to the 2:1 complex.

Fig. 6. Raman spectra of the $2\nu_8$ spectral region of 2-butyne (panel A) and infrared spectra of the $\nu_2+\nu_4$ spectral regions of $CF_3I$ for solutions of mixtures of $CF_3I$ with 2-butyne dissolved in liquid krypton at 120 K. Trace *a* in panel A shows the spectrum the mixed solution, while traces *b* and *c* refer to the solution containing only 2-butyne and $CF_3I$, respectively. Traces *b* and *c* in panel B are switched and represent the spectrum of the monomers $CF_3I$ and 2-butyne, respectively. New bands due to the 1:1 complexes appearing in the

spectrum of the mixtures are marked with an asterisk (*). Bands marked with a circle (o) are assigned to the 2:1 complex, consisting of one 2-butyne molecule and two $CF_3I$ moieties.

Fig.7 Van 't Hoff plots for the halogen bonded complexes of $CF_3I$ with ethyne (A), propyne (B) and 2-butyne (1:1, C; 2:1, D) and for the complexes of $CF_3Br$ with propyne (E) and 2-butyne (F).

Fig. 8 Comparison of the experimental and MP2/aug-cc-pVTZ-PP calculated complexation enthalpies for the halogen bonded complexes of various alkene (ethene and propene), alkyne (ethyne, propyne and 2-butyne) and aromatic (benzene and toluene) model type systems with $CF_3X$ (with X = Br, I).

**Table 1.**

MP2/aug-cc-pVDZ(-PP) bond lengths, in Å, and bond angles, in degrees, for the complexes of $CF_3Cl$, $CF_3Br$ and $CF_3I$ with ethyne.[a]

| | $CF_3Cl$•ethyne | | $CF_3Br$•ethyne | | $CF_3I$•ethyne | |
|---|---|---|---|---|---|---|
| $CF_3X$ | | | | | | |
| $r_{CF}$ | 1.3441 | (0.0015) | 1.3456 | (0.0016) | 1.3489 | (0.0020) |
| $r_{CX}$ | 1.7537 | (-0.0012) | 1.9128 | (0.0005) | 2.1431 | (0.0009) |
| $\theta_{XCF}$ | 110.61 | (0.14) | 110.72 | (0.17) | 110.94 | (0.22) |
| Ethyne | | | | | | |
| $r_{C\equiv C}$ | 1.2311 | (0.0005) | 1.2314 | (0.0008) | 1.2318 | (0.0012) |
| $r_{CH}$ | 1.0749 | (0.0004) | 1.0751 | (0.0006) | 1.0753 | (0.0008) |
| $\theta_{HCC}$ | 179.83 | (-0.17) | 179.70 | (-0.30) | 179.52 | (-0.48) |
| Intermolecular | | | | | | |
| $r_{X\cdots\pi}$ | 3.45 | | 3.43 | | 3.51 | |
| $\theta_{CX\cdots\pi}$ | 179.95 | | 179.93 | | 179.99 | |

[a] The values in brackets are the changes induced by the complexation. The X···π interatomic distances $r_{X\cdots\pi}$ are obtained by calculating the distance between the interacting halogen atom and the midpoint of the carbon-carbon triple bond.

**Table 2**

MP2/aug-cc-pVDZ(-PP) bond lengths, in Å, and bond angles, in degrees, for the complexes of $CF_3Cl$, $CF_3Br$ and $CF_3I$ with propyne.[a]

| | $CF_3Cl$·propyne | | $CF_3Br$·propyne | | $CF_3I$·propyne | |
|---|---|---|---|---|---|---|
| $CF_3X$[b] | | | | | | |
| $r_{CF}$ | 1.3440 | (0.0015) | 1.3458 | (0.0018) | 1.3495 | (0.0025) |
| $r_{CX}$ | 1.7533 | (-0.0016) | 1.9131 | (0.0008) | 2.1441 | (0.0019) |
| $\theta_{XCF}$ | 110.68 | (0.20) | 110.77 | (0.23) | 111.02 | (0.30) |
| Propyne | | | | | | |
| $r_{C\equiv C}$ | 1.2333 | (0.0006) | 1.2338 | (0.0011) | 1.2344 | (0.0016) |
| $r_{C-C}$ | 1.4705 | (0.0005) | 1.4705 | (0.0005) | 1.4705 | (0.0005) |
| $r_{CH_a}$ | 1.0731 | (0.0003) | 1.0734 | (0.0006) | 1.0737 | (0.0009) |
| $r_{CH_b}$ | 1.0996 | (0.0001) | 1.0996 | (0.0001) | 1.0996 | (0.0001) |
| $\theta_{CCC}$ | 179.66 | (-0.34) | 179.78 | (-0.22) | 179.97 | (-0.03) |
| Intermolecular | | | | | | |
| $r_{X\cdots\pi}$ | 3.37 | | 3.33 | | 3.40 | |
| $\theta_{CX\cdots\pi}$ | 171.39 | | 173.93 | | 175.01 | |

[a] The values in brackets are the changes induced by the complexation. The X···π interatomic distances $r_{X\cdots\pi}$ are obtained by calculating the distance between the interacting halogen atom and the midpoint of the carbon-carbon triple bond. [b] Structural data for the F-atom in the vicinity of the propyne methyl group.

**Table 3**

MP2/aug-cc-pVDZ(-PP) bond lengths, in Å, and bond angles, in degrees, for the complexes of $CF_3Cl$, $CF_3Br$ and $CF_3I$ with 2-butyne[a].

| | $CF_3Cl$·2-butyne | | $CF_3Br$·2-butyne | | $CF_3I$·2-butyne | |
|---|---|---|---|---|---|---|
| $CF_3X$ | | | | | | |
| $r_{CF}$ | 1.3445 | (0.0020) | 1.3465 | (0.0025) | 1.3503 | (0.0033) |
| $r_{CX}$ | 1.7535 | (-0.0015) | 1.9139 | (0.0016) | 2.1457 | (0.0035) |
| $\theta_{XCF}$ | 110.70 | (0.23) | 110.82 | (0.27) | 111.08 | (0.37) |
| 2-butyne | | | | | | |
| $r_{C\equiv C}$ | 1.2350 | (0.0007) | 1.2355 | (0.0013) | 1.2364 | (0.0021) |
| $r_{C-C}$ | 1.4711 | (0.0002) | 1.4713 | (0.0004) | 1.4715 | (0.0006) |
| $r_{CH}$ | 1.0998 | (-0.0001) | 1.0999 | (0.0000) | 1.1000 | (0.0001) |
| $\theta_{CCC}$ | 179.81 | (-0.19) | 179.96 | (-0.04) | 179.46 | (-0.54) |
| Intermolecular | | | | | | |
| $r_{X\cdots\pi}$ | 3.26 | | 3.23 | | 3.29 | |
| $\theta_{CX\cdots\pi}$ | 179.36 | | 179.30 | | 179.95 | |

[a] The values in brackets are the changes induced by the complexation. The X···π interatomic distances $r_{X\cdots\pi}$ are obtained by calculating the distance between the interacting halogen atom and the midpoint of the carbon-carbon triple bond.

**Table 4**

Intermolecular distance $R_{eq} = R(X\cdots\pi)$ [a], in Å, ratios $R_p$ [b], penetration distances $d_P$ [b] and netto charge transfers [c] for the complexes of $CF_3X$ (X = Cl, Br, I) with ethyne, propyne and 2-butyne. For completeness, the MP2/aug-cc-pVDZ(-PP) and MP2/aug-cc-pVTZ(-PP) complexation energies in kJ $mol^{-1}$, ΔE(DZ) and ΔE(TZ), are also given.

| | $CF_3Cl$·ethyne | $CF_3Br$·ethyne | $CF_3I$·ethyne |
|---|---|---|---|
| $R_{eq} = R(X\cdots\pi)$ | 3.45 | 3.43 | 3.51 |
| $R_{VdW}$ | 3.50 | 3.65 | 3.85 |
| $R_P = R_{eq} / R_{VdW}$ | 0.97 | 0.94 | 0.91 |
| $d_P = R_{eq} - R_{VdW}$ | -0.05 | -0.22 | -0.34 |
| charge transfer | -0.026 | -0.039 | -0.056 |
| ΔE (DZ) | -5.6 | -8.1 | -10.3 |
| ΔE (TZ) | -6.1 | -8.4 | -10.8 |
| | $CF_3Cl$·propyne | $CF_3Br$·propyne | $CF_3I$·propyne |
| $R_{eq} = R(X\cdots\pi)$ | 3.37 | 3.33 | 3.40 |
| $R_{VdW}$ | 3.50 | 3.65 | 3.85 |
| $R_P = R_{eq} / R_{VdW}$ | 0.96 | 0.91 | 0.88 |
| $d_P = R_{eq} - R_{VdW}$ | -0.13 | -0.32 | -0.45 |
| charge transfer | -0.032 | -0.054 | -0.072 |
| ΔE (DZ) | -8.3 | -11.5 | -14.7 |
| ΔE (TZ) | -9.1 | -12.0 | -15.4 |
| | $CF_3Cl$·2-butyne | $CF_3Br$·2-butyne | $CF_3I$·2-butyne |
| $R_{eq} = R(X\cdots\pi)$ | 3.26 | 3.23 | 3.29 |
| $R_{VdW}$ | 3.50 | 3.65 | 3.85 |
| $R_P = R_{eq} / R_{VdW}$ | 0.93 | 0.88 | 0.85 |
| $d_P = R_{eq} - R_{VdW}$ | -0.24 | -0.42 | -0.56 |
| charge transfer | -0.044 | -0.063 | -0.094 |
| ΔE (DZ) | -10.5 | -14.5 | -19.0 |
| ΔE (TZ) | -11.7 | -15.3 | -20.0 |

[a] The interatomic distances are obtained by calculating the distance between the interacting halogen atom and the midpoint of the carbon-carbon triple bond. [b] The values for the van der Waals radii used to calculate $R_{VdW}$ , $R_P$ and $d_P$ are 1.70 Å for C, 1.80 Å for Cl, 1.95 Å for Br and 2.15 Å for I. [c] The netto charge are based on CHELPG partial charges.

**Table 5**

Selected harmonic MP2/aug-cc-pVDZ(-PP) vibrational frequencies, in $cm^{-1}$, and infrared intensities, in km $mol^{-1}$, for the halogen bonded complexes of ethyne with $CF_3Cl$, $CF_3Br$ and $CF_3I$.

| Mode | $\nu_{monomer}$ | IR intensity | $\nu_{complex}$ | IR intensity | $\Delta\nu$ |
|---|---|---|---|---|---|
| $CF_3Cl$ | | | | | |
| $\nu_1$ | 1097.0 | 469.7 | 1099.0 | 511.6 | 2.0 |
| $\nu_3$ | 480.3 | 0.1 | 479.6 | 0.9 | -0.7 |
| $\nu_4$ | 1192.2 | 282.1 | 1186.8 | 279.4 | -5.3 |
| Ethyne | | | | | |
| $\nu_2$ | 1949.6 | 0 | 1946.7 | 0.3 | -2.9 |
| $CF_3Br$ | | | | | |
| $\nu_1$ | 1078.6 | 496.1 | 1081.6 | 536.7 | 2.9 |
| $\nu_3$ | 361.5 | 0.0 | 359.4 | 0.9 | -2.1 |
| $\nu_4$ | 1178.8 | 254.7 | 1173.3 | 254.8 | -5.5 |
| Ethyne | | | | | |
| $\nu_2$ | 1949.6 | 0 | 1945.2 | 0.7 | -4.4 |
| $CF_3I$ | | | | | |
| $\nu_1$ | 1060.0 | 546.9 | 1065.1 | 583.8 | 5.1 |
| $\nu_3$ | 295.1 | 0.3 | 293.0 | 2.2 | -2.1 |
| $\nu_4$ | 1162.0 | 227.6 | 1154.9 | 229.0 | -7.1 |
| Ethyne | | | | | |
| $\nu_2$ | 1949.6 | 0 | 1943.6 | 1.7 | -6.0 |

**Table 6**

**S**elected harmonic MP2/aug-cc-pVDZ(-PP) vibrational frequencies, in $cm^{-1}$, and infrared intensities, in km $mol^{-1}$, for the halogen bonded complexes of propyne with $CF_3Cl$, $CF_3Br$ and $CF_3I$.

| Mode | $\nu_{monomer}$ | IR intensity | $\nu_{complex}$ | IR intensity | $\Delta\nu$ |
|---|---|---|---|---|---|
| $CF_3Cl$ | | | | | |
| $\nu_1$ | 1097.0 | 469.7 | 1099.5 | 522.6 | 2.5 |
| $\nu_3$ | 480.3 | 0.1 | 479.6 | 1.3 | -0.8 |
| $\nu_4$ | 1192.2 | 282.1 | 1185.8 | 274.5 | -6.4 |
| propyne | | | | | |
| $\nu_3$ | 2127.5 | 3.4 | 2123.6 | 2.7 | -3.8 |
| $CF_3Br$ | | | | | |
| $\nu_1$ | 1078.6 | 496.1 | 1082.0 | 547.9 | 3.4 |
| $\nu_3$ | 361.5 | 0.0 | 358.5 | 1.4 | -3.0 |
| $\nu_4$ | 1178.8 | 254.7 | 1171.7 | 251.2 | -7.2 |
| propyne | | | | | |
| $\nu_3$ | 2127.5 | 3.4 | 2121.2 | 3.3 | -6.3 |
| $CF_3I$ | | | | | |
| $\nu_1$ | 1060.0 | 546.9 | 1066.1 | 595.5 | 6.1 |
| $\nu_3$ | 295.1 | 0.3 | 291.8 | 3.0 | -3.3 |
| $\nu_4$ | 1162.0 | 227.6 | 1152.4 | 226.5 | -9.6 |
| propyne | | | | | |
| $\nu_3$ | 2127.5 | 3.4 | 2118.3 | 5.1 | -9.2 |

**Table 7**

Selected harmonic MP2/aug-cc-pVDZ(-PP) vibrational frequencies, in $cm^{-1}$, and infrared intensities, in km $mol^{-1}$, for the halogen bonded complexes of 2-butyne with $CF_3Cl$, $CF_3Br$ and $CF_3I$.

| Mode | $\nu_{monomer}$ | IR intensity | $\nu_{complex}$ | IR intensity | $\Delta\nu$ |
|---|---|---|---|---|---|
| $CF_3Cl$ | | | | | |
| $\nu_1$ | 1097.0 | 469.7 | 1099.6 | 539.6 | 2.6 |
| $\nu_3$ | 480.3 | 0.1 | 479.0 | 1.9 | -1.4 |
| $\nu_4$ | 1192.2 | 282.1 | 1184.8 | 267.2 | -7.4 |
| 2-butyne | | | | | |
| $\nu_2$ | 2265.7 | 0 | 2261.2 | 0.4 | -4.5 |
| $CF_3Br$ | | | | | |
| $\nu_1$ | 1078.6 | 496.1 | 1082.6 | 559.2 | 4.0 |
| $\nu_3$ | 361.5 | 0.0 | 357.0 | 2.1 | -4.5 |
| $\nu_4$ | 1178.8 | 254.7 | 1169.9 | 248.0 | -8.9 |
| 2-butyne | | | | | |
| $\nu_2$ | 2265.7 | 0 | 2258.0 | 1.6 | -7.7 |
| $CF_3I$ | | | | | |
| $\nu_1$ | 1060.0 | 546.9 | 1067.1 | 598.0 | 7.1 |
| $\nu_3$ | 295.1 | 0.3 | 290.0 | 3.8 | -5.1 |
| $\nu_4$ | 1162.0 | 227.6 | 1150.0 | 224.0 | -12.0 |
| 2-butyne | | | | | |
| $\nu_2$ | 2265.7 | 0 | 2253.5 | 4.7 | -12.2 |

**Table 8**

Characteristic vibrational frequencies and complexation shifts, in $cm^{-1}$, for the 1:1 and 2:1 complexes of $CF_3I$ with 2-butyne. The experimental data refer to a solution in liquid krypton, at 120 K. The calculated values were derived from the MP2/aug-cc-pVDZ-PP harmonic vibrational frequencies.

| | | Calculated | Experiment |
|---|---|---|---|
| $\nu_2$ | 2-butyne | 2265.7 | 2247.8 |
| | 2-butyne· $CF_3I$ | 2253.5 (-12.2) | 2237.6 (-10.2) |
| | 2-butyne·$2CF_3I$ | 2240.1 (-25.6) | 2229.2 (-18.6) |
| $2\nu_8$ | 2-butyne | 2380.8 | 2324.3 |
| | 2-butyne·$CF_3I$ | 2370.2 (-10.6) | 2314.7 (-9.6) |
| | 2-butyne·$2CF_3I$ | 2360.2 (-20.6) | 2306.3 (-18.0) |
| $\nu_2 + \nu_4$ | $CF_3I$ | 1884.3 | 1909.9 |
| | 2-butyne·$CF_3I$ | 1868.3 (-16.0) | 1894.2 (-15.7) |
| | 2-butyne·$2CF_3I$ | 1873.0 (-11.3) | 1898.8 (-11.1) |

**Table 9**

MP2/aug-cc-pVTZ(-PP) complexation energies and complexation enthalpies for the complexes for the trifluorohalomethanes with ethyne, propyne and 2-butyne. The vapor phase complexation enthalpies $\Delta H°$(vap,calc) were obtained by combining the complexation energies with results from statistical thermodynamical calculations. The solution data were derived by combining the vapor phase complexation enthalpies with thermodynamical data on the solvent effects estimated from Monte Carlo Free Energy Perturbation (MC-FEP) simulations. For completeness, the experimental values determined in LKr are also given.

| | ethyne | | | propyne | | | 2-butyne | | | |
|---|---|---|---|---|---|---|---|---|---|---|
| | $CF_3Cl$ | $CF_3Br$ | $CF_3I$ | $CF_3Cl$ | $CF_3Br$ | $CF_3I$ | $CF_3Cl$ | $CF_3Br$ | $CF_3I$ | $2CF_3I$ |
| $\Delta E$ (calc) | -6,1 | -8,4 | -10,8 | -9,1 | -12,0 | -15,4 | -11,7 | -15,3 | -20,0 | -39,5 |
| $\Delta H°$ (vap,calc) | -5,0 | -7,3 | -9,7 | -6,9 | -9,9 | -13,3 | -9,6 | -13,2 | -18,0 | -35,4 |
| $\Delta H°$ (LKr,calc) | -4,1 | -6,0 | -8,8 | -4,8 | -7,8 | -11,6 | -7,7 | -10,9 | -15,4 | -29,3 |
| Experimental | | | | | | | | | | |
| $\Delta H°$ (LKr) | / | / | -5,9(3) | / | -5,6(3) | -8,1(2) | / | -7,3(2) | -10,9(2) | -20,9(7) |

**Table 10**

Experimental vibrational frequencies and complexation shifts, in $cm^{-1}$, for the complex of $CF_3I$ with ethyne dissolved in LKr at 120 K. The ab initio complexation shifts are derived from the MP2/aug-cc-pVDZ-PP harmonic vibrational frequencies.

| | Assignment | $\nu_{monomer}$ | $\nu_{complex}$ | $\Delta\nu_{exp}$ | $\Delta\nu_{calc}$ |
|---|---|---|---|---|---|
| $CF_3I$ | $\nu_2 + \nu_4$ | 1910.1 | 1909.8 | -0.3 | -8.9 |
| | $2\nu_2 + \nu_3$ | 1763.9 | 1763.4 | -0.5 | -5.7 |
| | $\nu_2 + \nu_5$ | 1280.3 | 1279.6 | -0.7 | -2.5 |
| | $\nu_2 + 2\nu_6$ | 1266.3 | 1265.6 | -0.7 | -0.4 |
| | $\nu_4$ | 1175.3 | 1168.5 | -6.8 | -7.1 |
| | $\nu_4$ ($^{13}C$) | 1142.8 | | | -7.1 |
| | $\nu_1$ | 1068.5 | | | 5.1 |
| | $\nu_1$ ($^{13}C$) | 1039.9 | | | 5.1 |
| | $\nu_2 + \nu_3$ | 1025.5 | | | -3.9 |
| | $\nu_2 + \nu_6$ | 1005.7 | 1005.2 | -0.5 | -1.1 |
| | $\nu_2$ | 740.0 | | | -1.8 |
| | $2\nu_3$ | 571.3 | | | -4.2 |
| | $\nu_5$ | 540.1 | 539.0 | -1.1 | -0.7 |
| | $2\nu_6$ | 526.6 | | | 1.4 |
| Ethyne | $\nu_2 + \nu_4 + \nu_5$ | 3285.8 | 3285.0 | -0.8 | -4.3 |
| | $\nu_3$ | 3272.5 | 3268.0 | -4.5 | -7.8 |
| | $\nu_2 + \nu_5$ | 2700.1 | | | -1.5 |
| | $3\nu_5$ | 2172.3 | | | 13.5 |
| | $\nu_2$ | 1970.1 | 1966.5 | -3.6 | -6.0 |
| | $2\nu_4 + \nu_5$ | 1936.4 | | | -1.1 |
| | $\nu_4 + \nu_5$ | 1325.4 | | | 1.7 |
| | $\nu_5$ | 731.4 | | | 4.5 |

**Table 11**

Experimental vibrational frequencies and complexation shifts, in $cm^{-1}$, for the complex of $CF_3I$ with propyne dissolved in LKr at 120 K. The ab initio complexation shifts are derived from the MP2/aug-cc-pVDZ-PP harmonic vibrational frequencies.

| | Assignment | $\nu_{monomer}$ | $\nu_{complex}$ | $\Delta\nu_{exp}$ | $\Delta\nu_{calc}$ |
|---|---|---|---|---|---|
| $CF_3I$ | $2\nu_4$ | 2339,3 | 2309,4 | -29,9 | -19.2 |
| | $\nu_2 + \nu_4$ | 1909.9 | 1897.3 | -12.6 | -12.6 |
| | $\nu_4 + \nu_5$ | 1713.8 | 1704.2 | -9.6 | -10.6 |
| | $\nu_4 + 2\nu_6$ | 1700.4 | 1690.8 | -9.6 | -7.2 |
| | $\nu_2 + \nu_5$ | 1280.3 | 1279.0 | -1.3 | -4.0 |
| | $\nu_2 + 2\nu_6$ | 1266.3 | 1265.1 | -1.2 | -0.6 |
| | $\nu_4$ | 1175.4 | 1165.4 | -10.0 | -9.6 |
| | $\nu_4$ ($^{13}C$) | 1142.8 | 1132.8 | -10.0 | -9.6 |
| | $\nu_1$ | 1065.5 | 1072.6 | 7.1 | 6.1 |
| | $\nu_1$ ($^{13}C$) | 1039.9 | 1043.6 | 3.7 | 6.1 |
| | $\nu_2 + \nu_3$ | 1025.4 | 1021.4 | -4.0 | -6.3 |
| | $\nu_2 + \nu_6$ | 1005.7 | 1004.5 | -1.2 | -1.8 |
| | $\nu_2$ | 740.7 | 738.9 | -1.8 | -3.0 |
| | $\nu_2$($^{13}C$) | 734.8 | 733.0 | -1.8 | -3.0 |
| | $2\nu_3$ | 571.3 | 566.1 | -5.2 | -6.6 |
| | $\nu_5$ | 540.0 | 540.5 | 0.5 | -1.0 |
| | $2\nu_6$ | 526.6 | 527.2 | 0.6 | 2.4 |
| | $\nu_3$ | 288.6 | 285.9 | -2.7 | -3.3 |
| | $\nu_6$ | 268.3 | | | 1.2 |
| Propyne | $\nu_3 + 2\nu_9$ | 3369.1 | 3365.5 | -3.6 | -3.4 |
| | $\nu_1$ | 3325.4 | 3318.0 | -7.4 | -8.4 |
| | $\nu_1$ ($^{13}C$) | 3308.6 | 3301.9 | -6.7 | -8.4 |
| | $\nu_2$ | 2929.3 | 2929.8 | 0.5 | -0.2 |
| | $2\nu_7$ | 2864.7 | 2862.1 | -2.6 | -6.2 |
| | $\nu_3$ | 2136.7 | 2130.0 | -6.7 | -9.2 |
| | $\nu_7 + 2\nu_{10}$ | 2056.1 | 2056.4 | 0.3 | -4.6 |
| | $\nu_7$ | 1443.7 | 1442.3 | -1.4 | -3.2 |
| | $\nu_4$ | 1381.9 | 1382.4 | 0.5 | -0.9 |
| | $\nu_8$ | 1032.4 | | | -0.8 |
| | $\nu_5$ | 929.8 | 927.8 | -2.0 | -3.9 |
| | $\nu_9$ | 630.4 | 641.5 | 11.1 | 2.9 |
| | $\nu_{10}$ | 333.0 | 339.6 | 6.6 | -0.7 |

**Table 12**

Experimental vibrational frequencies and complexation shifts, in $cm^{-1}$, for the complex of $CF_3Br$ with propyne dissolved in LKr at 120 K. The ab initio complexation shifts are derived from the MP2/aug-cc-pVDZ-PP harmonic vibrational frequencies.

| | Assignment | $\nu_{monomer}$ | $\nu_{complex}$ | $\Delta\nu_{exp}$ | $\Delta\nu_{calc}$ |
|---|---|---|---|---|---|
| $CF_3Br$ | $2\nu_4$ | 2375.3 | 2361.2 | -14.1 | -14.4 |
| | $2\nu_1$ | 2142.8 | 2149.9 | 7.1 | 6.8 |
| | $\nu_2 + \nu_4$ | 1951.2 | 1942.6 | -8.6 | -10.1 |
| | $\nu_2 + \nu_5$ | 1306 | | | -3.5 |
| | $\nu_4$ | 1198 | 1191.2 | -6.8 | -7.2 |
| | $\nu_4$ ($^{13}C$) | 1164.1 | 1157.6 | -6.5 | -7.2 |
| | $\nu_1$ | 1075 | 1078.4 | 3.4 | 3.4 |
| | $\nu_5 + \nu_6$ | 847.9 | 848.1 | 0.2 | 0.5 |
| | $\nu_2$ | 759.3 | 757.9 | -1.4 | -2.9 |
| | $\nu_5$ | 544.3 | 544.1 | -0.2 | -0.6 |
| Propyne | $\nu_3 + 2\nu_9$ | 3369.1 | | | -2.3 |
| | $\nu_1$ | 3325.4 | 3320.8 | -4.6 | -5.5 |
| | $\nu_1$ ($^{13}C$) | 3308.6 | | | -5.5 |
| | $\nu_2$ | 2929.3 | 2929.5 | 0.2 | -0.3 |
| | $2\nu_7$ | 2864.7 | 2863.5 | -1.2 | -5.0 |
| | $\nu_3$ | 2136.7 | 2133.3 | -3.4 | -6.3 |
| | $\nu_7 + 2\nu_{10}$ | 2056.1 | 2056.2 | 0.1 | -0.5 |
| | $\nu_7$ | 1443.7 | 1442.8 | -0.9 | -2.5 |
| | $\nu_4$ | 1381.9 | | | -0.7 |
| | $2\nu_9$ | 1247.4 | 1250.8 | 3.4 | 4.0 |
| | $\nu_8$ | 1032.4 | | | -0.7 |
| | $\nu_5$ | 929.8 | 928.6 | -1.2 | -3.0 |
| | $\nu_9$ | 633.7 | 637.2 | 3.5 | 2.0 |
| | $\nu_{10}$ | 333.0 | | | 1.0 |

**Table 13**

Experimental vibrational frequencies and complexation shifts, in $cm^{-1}$, for the 1:1 and 2:1 complexes of $CF_3I$ with 2-butyne dissolved in LKr at 120 K. The ab initio complexation shifts are derived from the MP2/aug-cc-pVDZ-PP harmonic vibrational frequencies.

| | Assignment | $\nu_{monomer}$ | $\nu_{complex}$ | $\Delta\nu_{exp}$ | $\Delta\nu_{calc}$ | $\Delta\nu_{exp}$ (2:1) | $\Delta\nu_{calc}$ (2:1) |
|---|---|---|---|---|---|---|---|
| $CF_3I$ | $2\nu_4$ | 2339.3 | 2305.1 | -34.2 | -24.0 | | |
| | $\nu_2 + \nu_4$ | 1909.9 | 1894.2 | -15.7 | -16.1 | -11.1 | -11.3 |
| | $\nu_4 + \nu_5$ | 1713.8 | 1701.6 | -12.2 | -13.4 | | |
| | $\nu_4 + 2\nu_6$ | 1700.4 | 1688.6 | -11.8 | -10.6 | | |
| | $\nu_4 + \nu_6$ | 1439.3 | 1437.3 | -2.0 | -11.3 | | |
| | $\nu_2 + \nu_5$ | 1280.3 | 1277.1 | -3.2 | -5.5 | | |
| | $\nu_2 + 2\nu_6$ | 1266.3 | 1264.0 | -2.3 | -2.7 | | |
| | $\nu_4$ | 1175.4 | 1163.0 | -12.4 | -12.0 | | |
| | $\nu_4$ ($^{13}C$) | 1142.8 | 1130.5 | -12.3 | -12.0 | | |
| | $\nu_1$ | 1065.5 | 1073.6 | 8.1 | 7.1 | | |
| | $\nu_1$ ($^{13}C$) | 1039.9 | 1044.2 | 4.3 | 7.1 | | |
| | $\nu_2 + \nu_3$ | 1025.4 | 1019.3 | -6.1 | -9.2 | | |
| | $\nu_2 + \nu_6$ | 1005.7 | 1003.6 | -2.1 | -3.4 | | |
| | $\nu_5 + \nu_6$ | 787.6 | 789.1 | 1.5 | -0.7 | | |
| | $\nu_2$ | 740.7 | 737.7 | -3.0 | -4.1 | | |
| | $\nu_2$ ($^{13}C$) | 734.8 | 732.1 | -2.7 | -4.1 | | |
| | $2\nu_3$ | 571.3 | 563.9 | -7.4 | -10.2 | | |
| | $\nu_5$ | 540.0 | 539.2 | -0.8 | -1.4 | | |
| | $2\nu_6$ | 526.6 | 527.2 | 0.6 | 1.4 | | |
| | $\nu_3$ | 288.6 | 285.2 | -3.4 | -5.1 | | |
| | $\nu_6$ | 268.3 | | | 0.7 | | |
| 2-butyne | $\nu_9$ | 2963.3 | 2966.2 | 2.9 | 2.3 | | |
| | $\nu_1$ | 2926.6 | 2922.4 | -4.2 | 0.4 | | |
| | $\nu_6$ | 2926.8 | 2926.5 | -0.3 | 0.5 | | |
| | $\nu_{10} + \nu_{14}$ | 2867.7 | 2865.8 | -1.9 | -6.4 | | |
| | $\nu_3 + \nu_7$ | 2738.5 | 2739.4 | 0.9 | -2.7 | | |
| | $2\nu_8$ | 2324.3 | 2314.7 | -9.6 | -10.6 | -18.0 | -20.6 |
| | $\nu_2$ | 2247.8 | 2237.6 | -10.2 | -12.2 | -18.6 | -25.6 |
| | $\nu_{11} + \nu_{15}$ | 2055.7 | | | -3.8 | | |
| | $\nu_{14}$ | 1445.3 | | | -4.0 | | |
| | $\nu_{10}$ | 1445.9 | 1437.3 | | -2.4 | | |
| | $2\nu_4$ | 1385.8 | 1387.3 | 1.5 | -5.4 | | |
| | $\nu_7$ | 1378.3 | 1379.1 | 0.8 | -1.7 | | |
| | $\nu_3$ | 1377.2 | 1377.7 | 0.5 | -1.0 | | |

| | | | | |
|---|---|---|---|---|
| $v_8$ | 1152.7 | | | -5.3 |
| $v_{11}$ | 1037.0 | | | 6.8 |
| $v_{15}$ | 1027.5 | | | -10.6 |
| $2v_{16}$ | 769.1 | 772.3 | 3.2 | -3.2 |
| $v_4$ | 694.9 | 694.6 | -0.3 | -2.7 |
| $v_{16}$ | 372.7 | 376.4 | 3.7 | -1.6 |
| $v_{12}$ | | 219.7 | | 11.1 |

**Table 14**

Experimental vibrational frequencies and complexation shifts, in $cm^{-1}$, for the complex of $CF_3Br$ with 2-butyne dissolved in LKr at 120 K. The ab initio complexation shifts are derived from the MP2/aug-cc-pVDZ-PP harmonic vibrational frequencies.

| | Assignment | $\nu_{monomer}$ | $\nu_{complex}$ | $\Delta\nu_{exp}$ | $\Delta\nu_{calc}$ |
|---|---|---|---|---|---|
| $CF_3Br$ | $2\nu_4$ | 2375.3 | 2357.8 | -17.5 | -17.8 |
| | $\nu_1 + \nu_4$ | 2268.3 | 2263.1 | -5.2 | -4.9 |
| | $2\nu_1$ | 2142.8 | 2151.1 | 8.3 | 8.0 |
| | $\nu_2 + \nu_4$ | 1951.2 | 1940.1 | -11.1 | -12.7 |
| | $\nu_4 + \nu_5$ | 1742.9 | 1733.7 | -9.2 | -9.7 |
| | $\nu_4$ | 1198.1 | 1189.4 | -8.7 | -8.9 |
| | $\nu_4$ ($^{13}C$) | 1164.1 | 1155.7 | -8.4 | -8.9 |
| | $\nu_2 + \nu_3$ ($^{81}Br$) | 1114.4 | 1110.9 | -3.5 | -8.3 |
| | $2\nu_5$ | 1093.0 | 1092.0 | -1.0 | -1.6 |
| | $\nu_1$ | 1075.1 | 1079.0 | 3.9 | 4.0 |
| | $\nu_5 + \nu_6$ | 847.9 | 848.3 | 0.4 | 0.4 |
| | $\nu_2$ | 759.3 | 757.0 | -2.3 | -3.8 |
| | $\nu_5$ | 544.3 | 543.8 | -0.5 | -0.8 |
| 2-butyne | $\nu_{13}$ | 2964.4 | | | 1.9 |
| | $\nu_9$ | 2963.3 | 2966.0 | 2.7 | 0.9 |
| | $\nu_1$ | 2926.6 | | | 0.1 |
| | $\nu_6$ | 2926.8 | | | 0.1 |
| | $\nu_{10} + \nu_{14}$ | 2867.7 | 2866.0 | -1.7 | -4.6 |
| | $\nu_3 + \nu_7$ | 2738.5 | 2739.1 | 0.6 | -2.0 |
| | $2\nu_8$ | 2324.3 | 2319.3 | -5.0 | -7.0 |
| | $\nu_2$ | 2247.8 | 2242.6 | -5.2 | -7.7 |
| | $\nu_{11} + \nu_{15}$ | 2055.7 | | | -3.4 |
| | $\nu_{14}$ | 1445.3 | | | -3.1 |
| | $\nu_{10}$ | 1445.9 | 1443.9 | -2.0 | -1.5 |
| | $2\nu_4$ | 1385.8 | | | -3.8 |
| | $\nu_7$ | 1378.3 | | | -1.3 |
| | $\nu_3$ | 1377.2 | | | -0.7 |
| | $\nu_8$ | 1152.7 | | | -3.5 |
| | $\nu_{11}$ | 1037.0 | | | 6.9 |
| | $\nu_{15}$ | 1027.5 | | | -10.3 |
| | $2\nu_{16}$ | 769.1 | | | 3.4 |
| | $\nu_4$ | 694.9 | | | -1.9 |
| | $\nu_{16}$ | 372.6 | 376.1 | 3.5 | 1.7 |

# A cryospectroscopic infrared and Raman study of the C-X···π halogen bonding motif : complexes of the $CF_3Cl$ , $CF_3Br$ , and $CF_3I$ with ethyne , propyne and 2-butyne.

N. Nagels, W.A. Herrebout *

Department of Chemistry, University of Antwerp, Groenenborgerlaan 171,

B-2020 Antwerp, Belgium

## Supporting Information

* corresponding author.

*Tel.* +32-3-2653373 , Fax. +32-3-2653205,

*Email address:* wouter.herrebout@ua.ac.be

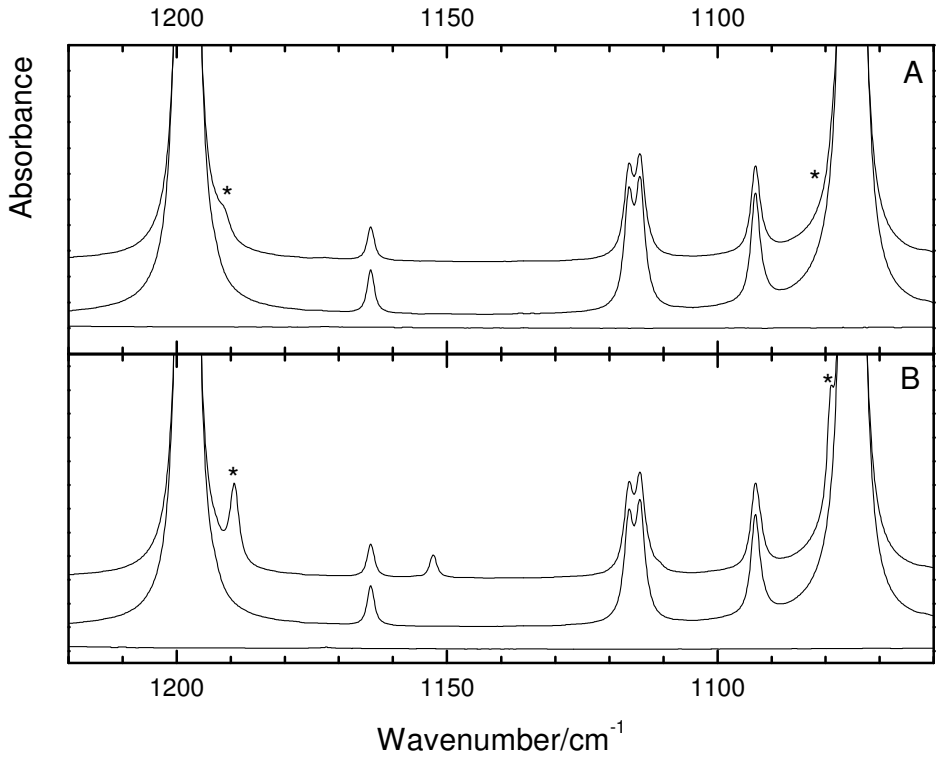


**Fig. S1**

Infrared spectra in the 1220-1060 $cm^{-1}$ spectral region for solutions in liquid krypton, at 120K, containing mixtures of $CF_3Br$ with propyne (panel A) and 2-butyne (panel B). Mole fractions of 1.9 x $10^{-4}$ of $CF_3Br$ and 1.9 × $10^{-3}$ of propyne (panel A) or 1.9 × $10^{-3}$ of 2-butyne (panel B) were used. In each panel the top trace represents the mixed solution, while the middle and bottom traces show the solution containing only $CF_3Br$ and propyne or 2-butyne, respectively. New bands due to 1:1 complex appearing in the spectrum of the mixtures are marked with an asterisk (*). In panel A, a weak band assigned to the antisymmetric $\nu_4$ stretching modes of $CF_3Br$ in the complex, is clearly visible at 1191.2 $cm^{-1}$. Another weak complex band, not immediately obvious, was observed at 1078.4 $cm^{-1}$ and is assigned to the symmetric $\nu_1$ stretching mode of $CF_3Br$. For the 2-butyne mixture, presented in panel B, the corresponding complex bands can be observed at 1189.4 and 1079.0 $cm^{-1}$, respectively. Using higher concentrations of $CF_3Br$, reveals the $^{13}C$-isotopomer complex bands of the $\nu_4$ stretching modes of $CF_3Br$ at 1157.6 $cm^{-1}$ and 1155.7 $cm^{-1}$ for propyne and 2-butyne, respectively.

**Table S1**

MP2/aug-cc-pVDZ vibrational frequencies, in $cm^{-1}$, and infrared intensities, in km $mol^{-1}$, for $CF_3Cl$·ethyne.

| Mode | $\nu_{monomer}$ | IR Intensity | $\nu_{complex}$ | IR Intensity | $\Delta\nu$ |
|---|---|---|---|---|---|
| $CF_3Cl$ | | | | | |
| $\nu_1$ ($a_1$) | 1097.0 | 469.7 | 1099.0 | 511.6 | 2.0 |
| $\nu_2$ ($a_1$) | 765.0 | 24.5 | 763.1 | 19.5 | -1.8 |
| $\nu_3$ ($a_1$) | 480.3 | 0.1 | 479.6 | 0.9 | -0.7 |
| $\nu_4$ (e) | 1192.2 | 282.1 | 1186.8 | 279.4 | -5.3 |
| $\nu_5$ (e) | 546.0 | 1.4 | 545.8 | 1.5 | -0.1 |
| $\nu_6$ (e) | 347.2 | 0.002 | 348.5 | 0.004 | 1.4 |
| Ethyne | | | | | |
| $\nu_1$ ($S_{GG}$) | 3526.0 | 0.0 | 3522.3 | 0.3 | -3.7 |
| $\nu_2$ ($S_{GG}$) | 1949.6 | 0.0 | 1946.7 | 0.3 | -2.9 |
| $\nu_3$ ($S_{GU}$) | 3435.8 | 93.6 | 3432.1 | 96.9 | -3.7 |
| $\nu_4$ ($P_{IG}$) | 414.7 | 0.0 | 413.3 | 0.01 | -1.3 |
| $\nu_5$ ($P_{IU}$) | 708.3 | 94.5 | 710.3 | 103.7 | 2.0 |

Van der Waals vibrations: 56.3 $cm^{-1}$, 0.1 km $mol^{-1}$; 55.6 $cm^{-1}$, 0.1 km $mol^{-1}$; 27.7 $cm^{-1}$, 0.01 km $mol^{-1}$; 24.7 $cm^{-1}$, 0.1 km $mol^{-1}$; 6.7 $cm^{-1}$, 0.0 km $mol^{-1}$.

**Table S2**

MP2/aug-cc-pVDZ-PP vibrational frequencies, in $cm^{-1}$, and infrared intensities, in km $mol^{-1}$, for $CF_3Br$•ethyne.

| Mode | $\nu_{monomer}$ | IR Intensity | $\nu_{complex}$ | IR Intensity | $\Delta\nu$ |
|---|---|---|---|---|---|
| $CF_3Br$ | | | | | |
| $\nu_1$ ($a_1$) | 1078.6 | 496.1 | 1081.6 | 536.7 | 2.9 |
| $\nu_2$ ($a_1$) | 739.4 | 29.7 | 737.3 | 21.3 | -2.1 |
| $\nu_3$ ($a_1$) | 361.5 | 0.04 | 359.4 | 0.9 | -2.1 |
| $\nu_4$ (e) | 1178.8 | 254.7 | 1173.3 | 254.8 | -5.5 |
| $\nu_5$ (e) | 531.3 | 0.9 | 530.9 | 1.1 | -0.4 |
| $\nu_6$ (e) | 305.8 | 0.01 | 306.7 | 0.002 | 0.9 |
| Ethyne | | | | | |
| $\nu_1$ ($S_{GG}$) | 3526.0 | 0.0 | 3520.4 | 0.5 | -5.5 |
| $\nu_2$ ($S_{GG}$) | 1949.6 | 0.0 | 1945.2 | 0.7 | -4.4 |
| $\nu_3$ ($S_{GU}$) | 3435.8 | 93.6 | 3430.2 | 99.9 | -5.5 |
| $\nu_4$ ($P_{IG}$) | 414.7 | 0.0 | 412.9 | 0.01 | -1.8 |
| $\nu_5$ ($P_{IU}$) | 708.3 | 94.5 | 711.5 | 108.1 | 3.2 |

Van der Waals vibrations: 68.3 $cm^{-1}$, 0.2 km $mol^{-1}$; 64.2 $cm^{-1}$, 0.5 km $mol^{-1}$; 28.9 $cm^{-1}$, 0.01 km $mol^{-1}$; 27.4 $cm^{-1}$, 0.03 km $mol^{-1}$; 1.8 $cm^{-1}$, 0.0 km $mol^{-1}$.

**Table S3**

MP2/aug-cc-pVDZ-PP vibrational frequencies, in $cm^{-1}$, and infrared intensities, in km $mol^{-1}$, for $CF_3I$·ethyne.

| Mode | $\nu_{monomer}$ | IR Intensity | $\nu_{complex}$ | IR Intensity | $\Delta\nu$ |
|---|---|---|---|---|---|
| $CF_3I$ | | | | | |
| $\nu_1$ ($a_1$) | 1060.0 | 546.9 | 1065.1 | 583.8 | 5.1 |
| $\nu_2$ ($a_1$) | 722.3 | 34.4 | 720.6 | 1.7 | -1.8 |
| $\nu_3$ ($a_1$) | 295.1 | 0.3 | 293.0 | 2.2 | -2.1 |
| $\nu_4$ (e) | 1162.0 | 227.6 | 1154.9 | 229.0 | -7.1 |
| $\nu_5$ (e) | 518.9 | 0.5 | 518.2 | 0.7 | -0.7 |
| $\nu_6$ (e) | 269.1 | 0.03 | 269.8 | 0.0003 | 0.7 |
| Ethyne | | | | | |
| $\nu_1$ ($S_{GG}$) | 414.7 | 0.0 | 411.9 | 0.02 | -2.8 |
| $\nu_2$ ($S_{GG}$) | 708.3 | 94.5 | 712.8 | 123.0 | 4.5 |
| $\nu_3$($S_{GU}$) | 1949.6 | 0.0 | 1943.6 | 1.7 | -6.0 |
| $\nu_4$ ($P_{IG}$) | 3435.8 | 93.6 | 3428.0 | 102.6 | -7.8 |
| $\nu_5$ ($P_{IU}$) | 3526.0 | 0.0 | 3518.2 | 1.0 | -7.8 |

Van der Waals vibrations: 79.3 $cm^{-1}$, 0.3 km $mol^{-1}$; 68.4 $cm^{-1}$, 1.2 km $mol^{-1}$; 29.9 $cm^{-1}$, 0.003 km $mol^{-1}$; 29.1 $cm^{-1}$, 0.02 km $mol^{-1}$; 0.6 $cm^{-1}$, 0.0 km $mol^{-1}$.

**Table S4**

MP2/aug-cc-pVDZ vibrational frequencies, in $cm^{-1}$, and infrared intensities, in km $mol^{-1}$, for $CF_3Cl$·propyne.

| Mode | $\nu_{monomer}$ | IR Intensity | $\nu_{complex}$ | IR Intensity | $\Delta\nu$ |
|---|---|---|---|---|---|
| $CF_3Cl$ | | | | | |
| $\nu_1$ ($a_1$) | 1097.0 | 469.7 | 1099.5 | 522.6 | 2.5 |
| $\nu_2$ ($a_1$) | 765.0 | 24.5 | 762.9 | 21.0 | -2.1 |
| $\nu_3$ ($a_1$) | 480.3 | 0.1 | 479.6 | 1.3 | -0.8 |
| $\nu_4$ (e) | 1192.2 | 282.1 | 1185.8 | 274.5 | -6.4 |
| $\nu_5$ (e) | 546.0 | 1.4 | 545.8 | 1.8 | -0.1 |
| $\nu_6$ (e) | 347.2 | 0.002 | 348.9 | 0.002 | 1.7 |
| Propyne | | | | | |
| $\nu_1$ ($a_1$) | 3496.5 | 53.8 | 3493.2 | 56.1 | -3.3 |
| $\nu_2$ ($a_1$) | 3077.2 | 16.6 | 3076.7 | 12.5 | -0.5 |
| $\nu_3$ ($a_1$) | 2127.5 | 3.4 | 2123.6 | 2.7 | -3.8 |
| $\nu_4$ ($a_1$) | 1396.2 | 0.3 | 1395.6 | 0.02 | -0.6 |
| $\nu_5$ ($a_1$) | 948.9 | 0.8 | 946.7 | 0.8 | -2.2 |
| $\nu_6$ (e) | 3170.1 | 5.3 | 3170.4 | 5.0 | 0.3 |
| $\nu_7$ (e) | 1472.0 | 7.9 | 1470.0 | 10.3 | -2.0 |
| $\nu_8$ (e) | 1044.4 | 0.01 | 1043.7 | 0.7 | -0.7 |
| $\nu_9$ (e) | 565.2 | 52.0 | 566.3 | 55.5 | 1.1 |
| $\nu_{10}$ (e) | 266.5 | 3.3 | 267.9 | 3.5 | 1.4 |

Van der Waals vibrations: 61.4 $cm^{-1}$, 0.7 km $mol^{-1}$; 54.2 $cm^{-1}$, 0.1 km $mol^{-1}$; 34.8 $cm^{-1}$, 0.04 km $mol^{-1}$; 24.3 $cm^{-1}$, 0.1 km $mol^{-1}$; 23.2 $cm^{-1}$, 0.3 km $mol^{-1}$; 2.2 $cm^{-1}$, 0.1 km $mol^{-1}$.

**Table S5**

MP2/aug-cc-pVDZ-PP vibrational frequencies, in $cm^{-1}$, and infrared intensities, in km $mol^{-1}$, for $CF_3Br$·propyne.

| Mode | $\nu_{monomer}$ | IR Intensity | $\nu_{complex}$ | IR Intensity | $\Delta\nu$ |
|---|---|---|---|---|---|
| $CF_3Br$ | | | | | |
| $\nu_1$ ($a_1$) | 1078.6 | 496.1 | 1082.0 | 547.9 | 3.4 |
| $\nu_2$ ($a_1$) | 739.4 | 29.7 | 736.6 | 25.4 | -2.9 |
| $\nu_3$ ($a_1$) | 361.5 | 0.0 | 358.5 | 1.4 | -3.0 |
| $\nu_4$ (e) | 1178.8 | 254.7 | 1171.7 | 251.2 | -7.2 |
| $\nu_5$ (e) | 531.3 | 0.9 | 530.7 | 1.2 | -0.6 |
| $\nu_6$ (e) | 305.8 | 0.0 | 306.9 | 0.0 | 1.1 |
| Propyne | | | | | |
| $\nu_1$ ($a_1$) | 3496.5 | 53.8 | 3490.9 | 57.9 | -5.5 |
| $\nu_2$ ($a_1$) | 3077.2 | 16.6 | 3076.8 | 11.0 | -0.3 |
| $\nu_3$ ($a_1$) | 2127.5 | 3.4 | 2121.2 | 3.3 | -6.3 |
| $\nu_4$ ($a_1$) | 1396.2 | 0.3 | 1395.5 | 0.0 | -0.7 |
| $\nu_5$ ($a_1$) | 948.9 | 0.8 | 945.9 | 1.0 | -3.0 |
| $\nu_6$ (e) | 3170.1 | 5.3 | 3171.1 | 4.4 | 1.0 |
| $\nu_7$ (e) | 1472.0 | 7.9 | 1469.6 | 10.8 | -2.5 |
| $\nu_8$ (e) | 1044.4 | 0.0 | 1043.7 | 0.8 | -0.7 |
| $\nu_9$ (e) | 565.2 | 52.0 | 567.2 | 58.3 | 2.0 |
| $\nu_{10}$ (e) | 266.5 | 3.3 | 267.5 | 3.7 | 1.0 |

Van der Waals vibrations: 72.4 $cm^{-1}$, 1.8 km $mol^{-1}$; 54.1 $cm^{-1}$, 0.1 km $mol^{-1}$; 38.9 $cm^{-1}$, 0.02 km $mol^{-1}$; 28.1 $cm^{-1}$, 0.06 km $mol^{-1}$; 26.0 $cm^{-1}$, 0.3 km $mol^{-1}$; 2.2 $cm^{-1}$, 0.1 km $mol^{-1}$.

**Table S6**

MP2/aug-cc-pVDZ-PP vibrational frequencies, in $cm^{-1}$, and infrared intensities, in km $mol^{-1}$, for $CF_3I$·propyne.

| Mode | $\nu_{monomer}$ | IR Intensity | $\nu_{complex}$ | IR Intensity | $\Delta\nu$ |
|---|---|---|---|---|---|
| $CF_3I$ | | | | | |
| $\nu_1$ ($a_1$) | 1060.0 | 546.9 | 1066.1 | 595.5 | 6.1 |
| $\nu_2$ ($a_1$) | 722.3 | 34.4 | 719.3 | 27.3 | -3.0 |
| $\nu_3$ ($a_1$) | 295.1 | 0.3 | 291.8 | 3.0 | -3.3 |
| $\nu_4$ (e) | 1162.0 | 227.6 | 1152.4 | 226.5 | -9.6 |
| $\nu_5$ (e) | 518.9 | 0.5 | 517.9 | 0.8 | -1.0 |
| $\nu_6$ (e) | 269.1 | 0.003 | 270.4 | 0.5 | 1.2 |
| Propyne | | | | | |
| $\nu_1$ ($a_1$) | 3496.5 | 53.8 | 3488.1 | 60.0 | -8.4 |
| $\nu_2$ ($a_1$) | 3077.2 | 16.6 | 3077.0 | 9.3 | -0.2 |
| $\nu_3$ ($a_1$) | 2127.5 | 3.4 | 2118.3 | 5.1 | -9.2 |
| $\nu_4$ ($a_1$) | 1396.2 | 0.3 | 1395.4 | 0.1 | -0.9 |
| $\nu_5$ ($a_1$) | 948.9 | 0.8 | 945.0 | 1.2 | -3.9 |
| $\nu_6$ (e) | 3170.1 | 5.3 | 3171.7 | 3.9 | 1.7 |
| $\nu_7$ (e) | 1472.0 | 7.9 | 1468.8 | 11.7 | -3.2 |
| $\nu_8$ (e) | 1044.4 | 0.01 | 1043.6 | 1.0 | -0.8 |
| $\nu_9$ (e) | 565.2 | 52.0 | 568.1 | 62.1 | 2.9 |
| $\nu_{10}$ (e) | 266.5 | 3.3 | 265.8 | 3.4 | -0.7 |

Van der Waals vibrations: 81.0 $cm^{-1}$, 3.9 km $mol^{-1}$; 57.4 $cm^{-1}$, 0.03 km $mol^{-1}$; 46.5 $cm^{-1}$, 0.002 km $mol^{-1}$; 32.6 $cm^{-1}$, 0.1 km $mol^{-1}$; 28.3 $cm^{-1}$, 0.2 km $mol^{-1}$; 2.1 $cm^{-1}$, 0.1 km $mol^{-1}$.

**Table S7**

MP2/aug-cc-pVDZ vibrational frequencies, in $cm^{-1}$, and infrared intensities, in km $mol^{-1}$, for $CF_3Cl$·2-butyne.

| Mode | $\nu_{monomer}$ | IR Intensity | $\nu_{complex}$ | IR Intensity | $\Delta\nu$ |
|---|---|---|---|---|---|
| $CF_3Cl$ | | | | | |
| $\nu_1$ ($a_1$) | 1097.0 | 469.7 | 1099.6 | 539.6 | 2.6 |
| $\nu_2$ ($a_1$) | 765.0 | 24.5 | 762.2 | 20.6 | -2.7 |
| $\nu_3$ ($a_1$) | 480.3 | 0.1 | 479.0 | 1.9 | -1.4 |
| $\nu_4$ (e) | 1192.2 | 282.1 | 1184.8 | 267.2 | -7.4 |
| $\nu_5$ (e) | 546.0 | 1.4 | 545.8 | 1.4 | -0.1 |
| $\nu_6$ (e) | 347.2 | 0.002 | 349.2 | 0.002 | 2.0 |
| 2-butyne | | | | | |
| $\nu_1$ ($A_{1G}$) | 3070.4 | 0.0 | 3069.4 | 0.04 | -1.0 |
| $\nu_2$ ($A_{1G}$) | 2265.7 | 0.0 | 2261.2 | 0.4 | -4.5 |
| $\nu_3$ ($A_{1G}$) | 1402.8 | 0.0 | 1402.7 | 0.01 | -0.1 |
| $\nu_4$ ($A_{1G}$) | 725.5 | 0.0 | 724.3 | 0.3 | -1.1 |
| $\nu_5$ ($A_{1U}$) | 24.5 | 0.0 | 20.5 | 0.01 | -4.0 |
| $\nu_6$ ($A_{2U}$) | 3071.1 | 58.4 | 3070.3 | 49.9 | -0.8 |
| $\nu_7$ ($A_{2U}$) | 1401.6 | 4.9 | 1400.9 | 2.0 | -0.6 |
| $\nu_8$ ($A_{2U}$) | 1190.4 | 0.2 | 1188.4 | 7.9 | -2.1 |
| $\nu_9$ (EU) | 3160.9 | 15.3 | 3160.3 | 14.0 | -0.6 |
| $\nu_{10}$ (EU) | 1476.1 | 13.8 | 1475.4 | 11.4 | -0.7 |
| $\nu_{11}$ (EU) | 1050.2 | 0.6 | 1057.4 | 2.2 | 7.1 |
| $\nu_{12}$ (EU) | 183.8 | 12.0 | 192.2 | 15.3 | 8.4 |
| $\nu_{13}$ (EG) | 3160.6 | 0.0 | 3161.1 | 0.1 | 0.5 |
| $\nu_{14}$ (EG) | 1475.8 | 0.0 | 1473.6 | 0.1 | -2.2 |
| $\nu_{15}$ (EG) | 1035.0 | 0.0 | 1025.4 | 0.02 | -9.6 |
| $\nu_{16}$ (EG) | 198.7 | 0.0 | 201.1 | 0.002 | 2.3 |

Van der Waals vibrations: 56.7 $cm^{-1}$, 0.03 km $mol^{-1}$; 55.7 $cm^{-1}$, 0.01 km $mol^{-1}$; 32.8 $cm^{-1}$, 0.001 km $mol^{-1}$; 23.0 $cm^{-1}$, 0.04 km $mol^{-1}$; 20.1 $cm^{-1}$, 0.01 km $mol^{-1}$;1.4 $cm^{-1}$, 0.0001 km $mol^{-1}$.

**Table S8**

MP2/aug-cc-pVDZ-PP vibrational frequencies, in $cm^{-1}$, and infrared intensities, in km $mol^{-1}$, for $CF_3Br$•2-butyne.

| Mode | $\nu_{monomer}$ | IR Intensity | $\nu_{complex}$ | IR Intensity | $\Delta\nu$ |
|---|---|---|---|---|---|
| $CF_3Br$ | | | | | |
| $\nu_1$ ($a_1$) | 1078.6 | 496.1 | 1082.6 | 559.2 | 4.0 |
| $\nu_2$ ($a_1$) | 739.4 | 29.7 | 735.6 | 24.3 | -3.8 |
| $\nu_3$ ($a_1$) | 361.5 | 0.04 | 357.0 | 2.1 | -4.5 |
| $\nu_4$ (e) | 1178.8 | 254.7 | 1169.9 | 248.0 | -8.9 |
| $\nu_5$ (e) | 531.3 | 0.9 | 530.5 | 1.0 | -0.8 |
| $\nu_6$ (e) | 305.8 | 0.01 | 307.0 | 0.002 | 1.2 |
| 2-butyne | | | | | |
| $\nu_1$ (A1G) | 3070.4 | 0.0 | 3070.7 | 0.4 | 0.4 |
| $\nu_2$ (A1G) | 2265.7 | 0.0 | 2253.5 | 4.7 | -12.2 |
| $\nu_3$ (A1G) | 1402.8 | 0.0 | 1401.8 | 0.3 | -1.0 |
| $\nu_4$ (A1G) | 725.5 | 0.0 | 722.7 | 0.4 | -2.7 |
| $\nu_5$ (A1U) | 24.5 | 0.0 | 38.6 | 0.0 | 14.2 |
| $\nu_6$ (A2U) | 3071.1 | 58.4 | 3071.6 | 35.8 | 0.5 |
| $\nu_7$ (A2U) | 1401.6 | 4.9 | 1399.9 | 0.8 | -1.7 |
| $\nu_8$ (A2U) | 1190.4 | 0.2 | 1185.1 | 0.9 | -5.3 |
| $\nu_9$ (EU) | 3160.9 | 15.3 | 3163.2 | 4.7 | 2.3 |
| $\nu_{10}$ (EU) | 1476.1 | 13.8 | 1473.7 | 19.9 | -2.4 |
| $\nu_{11}$ (EU) | 1050.2 | 0.6 | 1057.1 | 8.3 | 6.8 |
| $\nu_{12}$ (EU) | 183.8 | 12.0 | 194.9 | 21.3 | 11.1 |
| $\nu_{13}$ (EG) | 3160.6 | 0.0 | 3163.3 | 6.5 | 2.6 |
| $\nu_{14}$ (EG) | 1475.8 | 0.0 | 1471.8 | 0.3 | -4.0 |
| $\nu_{15}$ (EG) | 1035.0 | 0.0 | 1024.4 | 0.2 | -10.6 |
| $\nu_{16}$ (EG) | 198.7 | 0.0 | 197.1 | 0.1 | -1.6 |

Van der Waals vibrations: 60.7 $cm^{-1}$, 0.2 km $mol^{-1}$; 52.8 $cm^{-1}$, 0.02 km $mol^{-1}$; 36.6 $cm^{-1}$, 0.002 km $mol^{-1}$; 24.2 $cm^{-1}$, 0.1 km $mol^{-1}$; 8.8 $cm^{-1}$, 0.01 km $mol^{-1}$; 1.6 $cm^{-1}$, 0.0 km $mol^{-1}$.

**Table S9**

MP2/aug-cc-pVDZ-PP vibrational frequencies, in $cm^{-1}$, and infrared intensities, in km $mol^{-1}$, for $CF_3I$•2-butyne.

| Mode | $\nu_{monomer}$ | IR Intensity | $\nu_{complex}$ | IR Intensity | $\Delta\nu$ |
|---|---|---|---|---|---|
| $CF_3I$ | | | | | |
| $\nu_1$ ($a_1$) | 1060.0 | 546.9 | 1067.1 | 598.0 | 7.1 |
| $\nu_2$ ($a_1$) | 722.3 | 34.4 | 718.3 | 26.2 | -4.1 |
| $\nu_3$ ($a_1$) | 295.1 | 0.3 | 290.0 | 3.8 | -5.1 |
| $\nu_4$ (e) | 1162.0 | 227.6 | 1150.0 | 224.0 | -12.0 |
| $\nu_5$ (e) | 518.9 | 0.5 | 517.5 | 0.6 | -1.4 |
| $\nu_6$ (e) | 269.1 | 0.03 | 269.8 | 0.02 | 0.7 |
| 2-butyne | | | | | |
| $\nu_1$ ($A_1G$) | 3070.4 | 0.0 | 3070.7 | 0.4 | 0.4 |
| $\nu_2$ ($A_1G$) | 2265.7 | 0.0 | 2253.5 | 4.7 | -12.2 |
| $\nu_3$ ($A_1G$) | 1402.8 | 0.0 | 1401.8 | 0.3 | -1.0 |
| $\nu_4$ (A1G) | 725.5 | 0.0 | 722.7 | 0.4 | -2.7 |
| $\nu_5$ (A1U) | 24.5 | 0.0 | 38.6 | 0.0 | 14.2 |
| $\nu_6$ (A2U) | 3071.1 | 58.4 | 3071.6 | 35.8 | 0.5 |
| $\nu_7$ (A2U) | 1401.6 | 4.9 | 1399.9 | 0.8 | -1.7 |
| $\nu_8$ (A2U) | 1190.4 | 0.2 | 1185.1 | 0.9 | -5.3 |
| $\nu_9$ (EU) | 3160.9 | 15.3 | 3163.2 | 4.7 | 2.3 |
| $\nu_{10}$ (EU) | 1476.1 | 13.8 | 1473.7 | 19.9 | -2.4 |
| $\nu_{11}$ (EU) | 1050.2 | 0.6 | 1057.1 | 8.3 | 6.8 |
| $\nu_{12}$ (EU) | 183.8 | 12.0 | 194.9 | 21.3 | 11.1 |
| $\nu_{13}$ (EG) | 3160.6 | 0.0 | 3163.3 | 6.5 | 2.6 |
| $\nu_{14}$ (EG) | 1475.8 | 0.0 | 1471.8 | 0.3 | -4.0 |
| $\nu_{15}$ (EG) | 1035.0 | 0.0 | 1024.4 | 0.2 | -10.6 |
| $\nu_{16}$ (EG) | 198.7 | 0.0 | 197.1 | 0.1 | -1.6 |

Van der Waals vibrations: 65.4 $cm^{-1}$, 0.9 km $mol^{-1}$; 59.3 $cm^{-1}$, 0.04 km $mol^{-1}$; 43.6 $cm^{-1}$, 0.02 km $mol^{-1}$; 28.1 $cm^{-1}$, 0.1 km $mol^{-1}$; 28.1 $cm^{-1}$, 0.01 km $mol^{-1}$; 0.5 $cm^{-1}$, 0.0 km $mol^{-1}$.

**Table S10**

Comparison of the experimental frequencies of 2-butyne dissolved in liquid krypton at 120 K with literature data for the vapor and liquid phases and with the harmonic vibrational frequencies derived at the MP2/aug-cc-pVDZ (MP2/DZ) and MP2/aug-cc-pVTZ (MP2/TZ) levels.

| Assign | Sym | Coord | Gas | | Liquid | | LKr | | Calc | |
|---|---|---|---|---|---|---|---|---|---|---|
| | | | Raman | IR | Raman | IR | Raman | IR | MP2/DZ | MP2/TZ |
| $\nu_9$ | $E_{1u}$ | $q^-_{CH_3}(C-H)$ | | 2973 | | 2955 | | 2963.3 | 3160.9 | 3154.2 |
| $\nu_{13}$ | $E_{1g}$ | $q^-_{CH_3}(C-H)$ | 2966 | | 2961 | | 2964.4 | | 3160.6 | 3154.4 |
| $\nu_6$ | $A_{2u}$ | $q^+_{CH_3}(C-H)$ | | 2938 | | 2923 | | 2926.8 | 3071.1 | 3081.3 |
| $\nu_1$ | $A_{1g}$ | $q^+_{CH_3}(C-H)$ | 2916 | | 2920 | | 2926.6 | | 3070.4 | 3081.8 |
| $\nu_2$ | $A_{1g}$ | $Q$ (C≡C) | 2233 | | 2234.6 | | 2247.8 | | 2265.7 | 2303.2 |
| $\nu_{10}$ | $E_{1u}$ | $\alpha^-_{CH_3}$(HCH) | | 1456 | | 1444 | | 1445.9 | 1476.1 | 1511.5 |
| $\nu_{14}$ | $E_{1g}$ | $\alpha^-_{CH_3}$(HCH) | 1448 | | 1447 | | 1445.3 | | 1475.8 | 1508.7 |
| $\nu_7$ | $A_{2u}$ | $\alpha^+_{CH_3}$(HCH) | | 1382 | | 1374 | | 1378.3 | 1401.6 | 1411.9 |
| $\nu_3$ | $A_{1g}$ | $\alpha^+_{CH_3}$(HCH) | 1380 | | 1379 | | 1377.2 | | 1402.8 | 1420.0 |
| $\nu_8$ | $A_{2u}$ | $Q^-$ (C-C) | | 1152 | | 1141 | | 1152.7 | 1190.4 | 1187.2 |
| $\nu_{11}$ | $E_{1u}$ | $\beta_{CH_3}$(CCH) | | 1054 | | 1039 | | 1037 | 1050.2 | 1079.9 |
| $\nu_{15}$ | $E_{1g}$ | $\beta_{CH_3}$(CCH) | 1029 | | 1029 | | 1027.5 | | 1035.0 | 1054.9 |
| $\nu_4$ | $A_{1g}$ | $Q^+$ (C-C) | 693 | | 697.4 | | 694.9 | | 725.5 | 731.7 |
| $\nu_{16}$ | $E_{1g}$ | $\gamma$(C≡C-C) | 371 | | 374 | | 372.7 | | 198.7 | 354.6 |
| $\nu_{12}$ | $E_{1u}$ | $\gamma$(C≡C-C) | 213 | | 212 | 216[a] | | | 183.8 | 196.0 |
| $\nu_5$ | $A_{1u}$ | Free rotation of $CH_3$ | | | | | | | 24.5 | 20.5 |

[a] The weak line, observed in the Raman spectrum of the liquid, may be interpreted as the $\nu_{12}$ frequency appearing as a result of the slight breakdown of the $D_{6h}$ selection rules because of the molecular interaction in the liquid phase. [L. M. Sverdlov, M. A. Kovner and E. P. Krainov, *Vibrational Spectra of Polyatomic Molecules*, Halsted, New York, N. Y., **1973**]